# Interleukin 11 therapy causes acute left ventricular dysfunction

Mark Sweeney[1,2,3], Katie O'Fee[1,2], Chelsie Villanueva-Hayes[1,2],Ekhlas Rahman[1,2], Michael Lee[4], Chung Nga Tam[1], Eneko Pascual-Navarro[1,2], Henrike Maatz[5,6], Eric L. Lindberg[5], Konstantinos Vanezis[1,2,4], Chrishan J Ramachandra[7,8], Ivan Andrew[1,2], Emma R. Jennings[1,2], Wei-Wen Lim[7,8], Anissa A Widjaja[8], David Carling[1,2], Derek J Hausenloy[7,8,10,11], Norbert Hubner[5,6,9], Paul J.R. Barton[1,2,4,12], Stuart A Cook[1,2,7,8]

[1]MRC-Laborary of Medical Sciences, Hammersmith Hospital Campus, London, UK.

[2]Institute of Clinical Sciences, Faculty of Medicine, Imperial College London, London, UK.

[3]Wellcome Trust / NIHR 4i Clinical Research Fellow, Imperial College London, London, UK.

[4]National Heart and Lung Institute, Imperial College London, London, UK.

[5]Cardiovascular and Metabolic Sciences, Max Delbrück Center for Molecular Medicine in the Helmholtz Association (MDC), Berlin, Germany.

[6]DZHK (German Centre for Cardiovascular Research), Partner Site Berlin, Berlin, Germany.

[7]National Heart Research Institute Singapore, National Heart Centre Singapore, Singapore.

[8]Cardiovascular and Metabolic Disorders Program, Duke-National University of Singapore Medical School, Singapore.

[9]Charite, Universitätsmedizin Berlin, Berlin, Germany.

[10]Yong Loo Lin School of Medicine, National University of Singapore, Singapore, Singapore.

[11]The Hatter Cardiovascular Institute, University College London, London, UK.

[12]Royal Brompton and Harefield Hospitals, Guy's and St. Thomas' NHS Foundation Trust, London UK

**Short title:** Acute cardiac toxicities of interleukin 11

**Address for correspondence:**

Dr Mark Sweeney, London Institute of Medical Science, Imperial College London. W12 0NN. msweeney@ic.ac.uk or Professor Stuart Cook, London Institute of Medical Science, Imperial College London, W12 0NN. stuart.cook@imperial.ac.uk

**Category:** Original article

# Abstract

## Aims

Interleukin 11 (IL11) was initially thought important for platelet production, which led to recombinant IL11 being developed as a drug to treat thrombocytopenia. IL11 was later found to be redundant for haematopoiesis and its use in patients is associated with unexplained and severe cardiac side effects. Here we aim to identify, for the first time, direct cardiomyocyte toxicities associated with IL11, which was previously believed cardioprotective.

## Methods and Results

We injected recombinant mouse lL11 (rmIL11) into mice and studied its molecular effects in the heart using immunoblotting, qRT-PCR, bulk RNA-seq, single nuclei RNA-seq (snRNA-seq) and ATAC-seq. The physiological impact of IL11 was assessed by echocardiography *in vivo* and using cardiomyocyte contractility assays *in vitro*. To determine the activity of IL11 specifically in cardiomyocytes we made two cardiomyocyte-specific *Il11ra1* knockout (CMKO) mouse models using either AAV9-mediated and *Tnnt2*-restricted (vCMKO) or *Myh6* (m6CMKO) Cre expression and an *Il11ra1* floxed mouse strain. In pharmacologic studies, we studied the effects of JAK/STAT inhibition on rmIL11-induced cardiac toxicities. Injection of rmIL11 caused acute and dose-dependent impairment of left ventricular ejection fraction (saline: 62.4% ± 1.9; rmIL11: 32.6% ± 2.9, $p<0.001$, n=5). Following rmIL11 injection, myocardial STAT3 and JNK phosphorylation were increased and bulk RNA-seq revealed upregulation of pro-inflammatory pathways (TNFα, NFκB and JAK/STAT) and perturbed calcium handling. snRNA-seq showed rmIL11-induced expression of stress factors (*Ankrd1*, *Ankrd23*, *Xirp2*), activator protein-1 (AP-1) transcription

factor genes and *Nppb* in the cardiomyocyte compartment. Following rmIL11 injection, ATAC-seq identified the *Ankrd1* and *Nppb* genes and loci enriched for stress-responsive, AP-1 transcription factor binding sites. Cardiomyocyte-specific effects were examined in vCMKO and m6CMKO mice, which were both protected from rmIL11-induced left ventricular impairment and molecular pathobiologies. In mechanistic studies, inhibition of JAK/STAT signalling with either ruxolitinib or tofacitinib prevented rmIL11-induced cardiac dysfunction.

## Conclusions

Injection of IL11 directly activates IL11RA/JAK/STAT3 in cardiomyocytes to cause acute heart failure. Our data overturn the earlier assumption that IL11 is cardioprotective and explain the serious cardiac side effects associated with IL11 therapy.

# Translational Perspective

Injection of IL11 into mice causes acute and dose-dependent left ventricular impairment by activation of JAK/STAT3 signalling in cardiomyocytes which induces cell stress, inflammation and impaired calcium handling. These data identify, for the first time, that IL11 is directly toxic in cardiomyocytes, overturning the earlier literature that suggested the opposite.

Recombinant human IL11 (rhIL11) is used as a drug to increase platelets in patients with thrombocytopenia but this has severe and unexplained cardiac side effects that were previously believed sporadic and non-specific. These findings have translational implications as in combination with previously described side effects of rhIL11 in clinical practice they question the continued use of rhIL11 in patients around the world.

# Abbreviations

| | |
|---|---|
| **AAV9** | Adeno-associated virus serotype 9 |
| **ANOVA** | Analysis of variance |
| **AP-1** | Activator protein 1 |
| **ATAC** | Assay for transposase-accessible chromatin with sequencing |
| **CM** | Cardiomyocyte |
| **DNA** | Deoxyribonucleic acid |
| **EC** | Endothelial cells |
| **ECG** | Electrocardiogram |
| **EGFP** | Enhanced green florescent protein |
| **ERK** | Extracellular signal regulated kinase |
| **FDR** | False discovery rate |
| **FOSL2** | FOS like 2 |
| **GAPDH** | Glyceraldehyde-3-phosphate dehydrogenase |
| **GCS** | Global circumferential strain |
| **GSEA** | Gene set enrichment analysis |
| **IL6** | Interleukin 6 |
| **IL11** | Interleukin 11 |
| **IL11RA1** | Interleukin 11 receptor A1 |
| **IP** | Intraperitoneal |
| **JAK** | Janus kinase |
| **JNK** | c-Jun N-terminal kinase |
| **KEGG** | Kyoto encyclopaedia of genes and genomes |
| **LV** | Left ventricle |

| | |
|---|---|
| **LVEF** | Left ventricular ejection fraction |
| **PBS** | Phosphate buffered saline |
| **PCR** | Polymerase chain reaction |
| **PSAX** | Parasternal short axis |
| **QPCR** | Quantitative polymerase chain reaction |
| **rhIL11** | Recombinant human interleukin 11 |
| **RIPA** | Radioimmunoprecipitation assay buffer |
| **rmIL6** | Recombinant mouse interleukin 6 |
| **rmIL11** | Recombinant mouse interleukin 11 |
| **RNA** | Ribonucleic acid |
| **SEM** | Standard error of the mean |
| **STAT** | Signal transducer and activator of transcription |
| **TNF** | Tumour necrosis factor |
| **UMAP** | Uniform Manifold Approximation and Projection |
| **vCMKO** | Viral mediated cardiomyocyte *Il11ra1 knockout* |
| **VTI** | Velocity time integral |
| **WT** | Wild type |

# Introduction

Interleukin 11 (IL11) is an elusive member of the interleukin 6 (IL6) family of cytokines, which collectively signal via the gp130 co-receptor. Following its identification in 1990[1] recombinant human IL11 (rhIL11) was found to increase megakaryocyte activity and peripheral platelet counts in mice[2]. Soon after, IL11 was developed as a therapeutic (Oprelvekin; Neumega) to increase platelet counts in patients with chemotherapy-induced thrombocytopenia, received FDA approval for this indication in 1998, and is still used to this day[3,4]. In recent years, longer-acting formulations of rhIL11 have been tested in pre-clinical studies and new clinical trials of PEGylated rhIL11 in patients are anticipated[5].

RhIL11 was also trialled to increase platelet counts in patients with von Willebrand factor deficiency, myelodysplastic syndrome, cirrhosis and sepsis, and tested as a putative cytoprotective agent in numerous other conditions, including myocardial infarction[6] [**Table 1 and Suppl Table 1**]. However, it became apparent that IL11 is not required for basal or compensatory red blood cell or platelet production in mice or humans: IL11 is in fact redundant for haematopoiesis[7,8]. Thus, the effects of injection of high dose rhIL11 on platelets appear non-physiological and possibly reflect non-specific gp130 activity[9,10].

Unfortunately, injection of rhIL11 into patients has severe and hitherto unexplained cardiac side effects. Up to 20% of patients given rhIL11 (50 µg/kg) develop atrial arrhythmias, a high proportion of individuals develop heart failure and rare cases of ventricular arrhythmias and sudden death are reported[11,12]. Furthermore, serum natriuretic peptide levels become acutely and

transiently elevated in patients receiving IL11 therapy, with B-natriuretic peptide levels sometimes exceeding those diagnostic of heart failure.

While IL11 was previously thought to be cytoprotective, anti-inflammatory and anti-fibrotic in the heart[13–15] and other organs, recent studies by ourselves and others have challenged this premise[16–18]. Indeed, experiments over the last five years have questioned the earlier literature and IL11 is increasingly viewed as pro-inflammatory and pro-fibrotic. Given this large shift in our understanding of IL11 and the fact that cardiomyocytes (CMs) robustly express IL11 receptors IL11RA[15,19,20], we devised experiments to determine whether IL11 is toxic to CMs and if this could explain cardiac side effects associated with IL11 therapy in patients.

## Methods

Detailed information on experimental methods of RNA and DNA analysis and CM isolation is provided in the supplementary material.

### Animal studies

All mouse studies were conducted according to the Animals (Scientific Procedures) Act 1986 Amendment Regulations 2012 and approved by the Animal Welfare Ethical Review Body at Imperial College London. Animal experiments were carried out under UK Home Office Project License P108022D1 (September 2019). Wild type (WT) mice on a C57BL/6J background were purchased from Charles River (Cat#632). They were bred in a dedicated breeding facility and

housed in a single room of the experimental animal facility with a 12-hour light-dark cycle and provided food and water *ad libitum*. Mice were euthanised by cervical dislocation and decapitation prior to removal of tissue for analysis.

The *Il11ra1* floxed mouse (C57BL/6-Il11ra1$^{em1Cook}$/J, Jax:034465) has exons 4-7 of the *Il11ra1* gene flanked by loxP sites as has been described previously[21]. In the presence of Cre-recombinase excision of exon 4-7 results in a non-functional IL11 receptor.

Male myosin heavy chain 6 Cre (*Myh6*-Cre) mice (B6.FVB-Tg(Myh6-cre)2182Mds/J, Jax:011038) were purchased from Jax (Bar Harbor, Maine, United States) as heterozygotes. These mice were crossed with homozygous *Il11ra1* floxed females. In the second generation, mice from generation one, heterozygous for the *Il11ra1* flox allele and heterozygous for the Cre, were crossed with *Il11ra1* flox homozygotes to produce littermate experimental and control animals.

Recombinant mouse interleukin-11 (rmIL11) (Z03052, Genscript, Oxford, UK) was dissolved in phosphate-buffered saline (PBS) (14190144, ThermoFisher, MA, USA), and injected intraperitoneally (IP) at a dose of 200 µg/kg unless otherwise stated. Control mice received an equivalent volume of saline (2 µL/kg). Recombinant mouse interleukin-6 (Z02767, Genscript) was dissolved in PBS and injected IP at a dose of 200 µg/kg.

## Genotyping

Genotype was confirmed with ear-notch DNA samples. DNA was extracted using a sodium hydroxide digestion buffer, then neutralised with 1M Tris-HCl pH 8. *Il11ra1* flox genotype was confirmed with a single polymerase chain reaction (PCR) reaction yielding a PCR product at 163

bp for the wild type allele or 197 bp in the transgenic allele. *Myh6*-Cre mice were genotyped using two reactions for either the transgenic gene product of 295 bp (or wild type gene product of 300 bp) along with an internal positive control (200 bp). Primers used in these reactions are detailed in supplementary table 2.

## Viral Vector

The viral vector used in this study, AAV9-cTNT-EGFP-T2A-iCre-WPRE (VB5413), was purchased from Vector Biolabs (Malvern, PA, USA). A codon optimised Cre was delivered using an adeno-association virus type 9 (AAV9) capsid and under the control of the *Tnnt2* promoter. This was linked to an enhanced green fluorescent protein (EGFP) reporter with a 2a self-cleaving linker. $1x10^{12}$ genome copies or an equivalent volume of saline were injected into the tail veins of 8 - 9 week old homozygous male *Il11ra1* flox mice and from this point mice were housed separately from saline-injected controls for 4 weeks prior to further experiments.

## Echocardiography

Echocardiography was performed under light isoflurane anaesthesia using a Vevo3100 imaging system and MX550D linear transducer (Fujifilm Visualsonic Inc, ON, Canada). Anaesthesia was induced with 4% isoflurane for 1 minute and maintained with 1-2% isoflurane. Mice were allowed to equilibrate to the anaesthetic after induction for 9 minutes before imaging was started. Heart rate measurement from single-lead electrocardiogram (ECG) recordings were taken at the completion of the equilibration period. Measurements of ventricular ejection fraction (LVEF) were measured from m-mode images taken in the parasternal short axis (PSAX) view at mid-ventricular level and averaged across 3 heartbeats.

## qPCR

The tissue was washed in ice-cold PBS and snap-frozen in liquid nitrogen. Total RNA was extracted using TRIzol (15596026, Invitrogen, MA, USA,) in RNeasy columns (74106, Qiagen, MD, USA). cDNA was synthesised using Superscript Vilo Mastermix (11755050, Invitrogen). Gene expression analysis was performed using quantitative polymerase chain reaction (qPCR) with TaqMan gene expression assay in duplicate over 40 cycles. *Il11ra1*: custom TaqMan assay [**Suppl Table 3]**, *Nppb*: Mm01255770_g1, *Rrad*: Mm00451053_m1, *Fosl2* Mm00484442_m1. Gene expression data were normalised to *Gapdh* expression (Mm99999915_g1) and fold change compared to control samples was calculated using $2^{-\Delta\Delta Ct}$ method.

## RNASeq

8 week old male C57BL/6J mice were injected with rmIL11 (200 µg/kg) or an equivalent volume of saline (2 µL/kg). The left ventricle (LV) was excised and flash frozen 1, 3 or 6 hours after injection. Libraries were sequenced on a NextSeq 2000 to generate a minimum of 20 million paired end 60bp reads per sample.

Raw RNAseq data and gene-level counts have been uploaded onto the NCBI Gene Expression Omnibus database and will be made available upon acceptance with accession number (GSE240804).

## Single nuclei RNAseq

Single nuclei sequencing was performed on flash frozen LV tissue that was extracted from 8 week old male C57BL/6J mice 3 hours after injection with rmIL11 or saline. The tissue was

processed according to standard protocols as previously described[22,23]. Nuclei were purified by fluorescent activated cell sorting and libraries were sequenced using HiSeq 4000 (Illumina, CA, USA) with a minimum depth of 20,000–30,000 read pairs per nucleus.

All single nuclei sequence data generated and analyzed in this study have been deposited in the European Nucleotide Archive (ENA) at EMBL-EBI under accession number PRJEB67301 (https://www.ebi.ac.uk/ena/browser/view/PRJEB67301).

## ATAC Seq

8 week old male C57BL/6J mice were given an IP injection with rmIL11 (200 µg/kg) or saline. The heart was excised 3 hours after injection and flash-frozen tissue was sent to Active Motif to perform assay for transposase-accessible chromatin with sequencing (ATAC-seq) analysis.

## Protein Analysis

Protein extraction was performed on flash frozen tissue using ice-cold Pierce RIPA buffer (89901, ThermoFisher) supplemented with protease inhibitors (11697498001, Roche, Basel, Switzerland) and phosphatase inhibitors (4906845001, Roche). Tissue was lysed using a Qiagen Tissue Lyser II with metallic beads for 3 mins at 30Hz. Protein quantification was performed using a Pierce bicinchoninic acid assay colorimetric protein assay kit (23225, ThermoFisher). 10-20 µg of protein was loaded per well and run on a 4-12% bis-tris precast sodium-dodecyl sulfate page gel (NP0323BOX, Invitrogen). Semi-dry transfer was performed using the TransBlot Turbo transfer system (1704150, BioRad, CA, USA) and the membrane was blocked in 5% bovine serum albumin (A3803, Sigma-Aldrich, MO, USA). Primary antibodies raised against the following targets were used: signal transducer and activator of transcription 3 (STAT3) (4904S, Cell

signalling technology (CST), MA, USA), pSTAT3 Tyr705 (9145L, CST), Extracellular signal regulated kinase (ERK) (9101S, CST), pERK (4695S, CST), c-Jun-N-terminal kinase (JNK) (sc-7345, Santa-Cruz, TX, USA), phospho-JNK (sc-6254, Santa-Cruz), green fluorescent protein (ab290, Abcam) Glyceraldehyde-3-phosphate dehydrogenase (GAPDH) (2118L, CST). Appropriate secondary horseradish peroxidase linked antibody was incubated for 1 hour with gentle agitation at room temperature and developed using chemiluminescence blotting substrate (1705061, BioRad or 34095, Thermofisher, depending on strength of signal).

## Cardiomyocyte extraction

CMs were extracted from the heart of 12 week old male C57BL/6J mice. Cells were incubated in Tyrode solution (1 mM Ca, 1 mM Mg) or Tyrode solution supplemented with rmIL11 (10 ng/mL) for 2 hours before recording. Cells were paced at 1Hz (10 V, 10 ms pulse width). Cell recordings were made using the Cytocypher high-throughput microscope (Cytocypher BV, Netherlands) and the automated cell finding system was used to identify and take recordings from 20 individual cells per heart per experimental condition. Calcium recordings were performed by incubating CMs with Fura 2AM dye (1 uM) for 20 mins before fluorescent recordings were taken.

## Statistics

Statistical analyses were performed in GraphPad Prism V9.5.0 unless otherwise stated. Normality testing was performed using the Shapiro-Wilk test. Hypothesis testing for single comparisons was done using an unpaired two ways Student's t-test for normally distributed data or by Mann-Whitney U test for non-normally distributed data.

Comparisons involving male and female mice were performed using a two-way analysis of variance (ANOVA) with Sidak's multiple comparisons testing. Changes in expression over

multiple time points were analysed using a one-way ANOVA with Sidak's multiple comparisons testing for all timepoints and doses. All graphs display the mean and standard error of the mean unless stated otherwise. P-values in RNA seq analysis were corrected for multiple testing using the false discovery rate (FDR) approach. A p-value and FDR of <0.05 was considered significant.

## Hierarchical testing of nested data

Statistical analysis of the data from high throughput microscopy of extracted CM experiments were analysed using a hierarchical statistical approach[24]. This approach tests for clustering within the data as may occur due to differences in the quality of myocyte preparation on different days. This avoids pseudoreplication of multiple technical replicates of a single biological replicate but also increases statistical power compared to treating each biological extraction as a single replicate. This uses a two-level random intercept model of linear regression. The analysis was performed using R-studio and the data was presented as the mean and standard deviation and effective n number taking the intraclass clustering into account.

## Figures

Graphs were prepared in GraphPad Prism V9.5.0 and R studio (Version 2023.03.0) Illustrations were created with Biorender.com and Figures were arranged in Adobe Illustrator (Version 23.0.4.).

# Results

## Injection of rmIL11 to mice causes acute left ventricular dysfunction

To model the effects of IL11 injection in clinical practice and analyse the effects on cardiac function we injected male C57BL/6J mice intraperitoneally with rmIL11 (200 µg/kg). As compared to mice injected with saline (2 µL/kg), rmIL11 injected mice developed a sinus tachycardic (Saline: 410 beats per minute (bpm) ± 6.9; rmIL11: 544 bpm ± 13, Mann Whitney test: p=0.0079, n=5) [**Fig 1A, B]**. Mice injected with rmIL11 injection had reduced LVEF (Saline: 62.4% ± 1.9; rmIL11: 32.6% ± 2.9, p<0.001, n=5), reduced global circumferential strain (GCS) (Saline: -33.4% ± 1.3; rmIL11: -10.6% ± 0.6, p<0.001, n=5) and reduced velocity time integral (VTI) in the aortic arch (Saline: 39.4 mm ± 3.6; rmIL11: 20.2 mm ± 2.1, p<0.002, n=5) compared to mice injected with saline [**Fig 1C-F] [Table 2]**. To serve as a related cytokine control an equivalent dose (200 µg/kg) of recombinant mouse IL6 (rmIL6) was injected which had no detectable acute effects on cardiac function [**Fig 1A-F & Suppl Fig S1A, B] [Table 2]**.

Dosing studies revealed that the effects of rmIL11 on heart rate and LV function were dose-dependent, consistent with physiological binding to and activation of the IlL11RA1 receptor. Cardiac impairment was evident at low doses and near-maximal effects were seen with a dose of 50 µg/kg, which is the dose typically given daily to patients with thrombocytopenia post-chemotherapy [**Fig 1G].** The effect of rmIL11 was rapid with a nadir in cardiac function 2 hours post injection and recovery of LV function was seen by 24 hour post injection [**Fig 1H]**.

## IL11 causes impaired cardiomyocyte calcium handling

We next examined IL11 signalling pathways in cardiac extracts following rmIL11 injection, which revealed early and short-lived phosphorylation of signal transducer and activator of transcription 3 (p-STAT3) but no apparent ERK activation, which differs from acute signalling effects in the liver and other organs[25] [**Fig 1I & Suppl Fig S1C].** Phosphorylation of JNK is a stress-related signalling pathway shown to be elevated in the mouse liver following IL11 treatment[25]. In the myocardium, JNK was phosphorylated at the 3 hour time point post rmIL11 injection by which stage STAT3 phosphorylation was declining [**Fig 1I & & Suppl Fig S1D]**.

The effect of IL11 directly on CMs was analysed *in vitro* by treating isolated adult mouse CMs with rmIL11 for 2 hours. CMs treated with rmIL11 demonstrated reduced contractility, as compared to control cells (Control: 1.00 ± 0.18; rmIL11: 0.67 ± 0.15, $p<0.00027$) [**Fig 1J]**. Intracellular calcium transients revealed blunting of the peak calcium concentration during systole in the presence of rmIL11 (Control: 1.00 ± 0.097; rmIL11: 0.78 ± 0.086, $p<0.00019$) **[Fig 1K].**

**[Insert Figure 1]**

## IL11 causes cardiac inflammation

The robust and early activation of STAT3 by IL11 led us to explore transcriptional changes which might occur acutely within the myocardium in response to IL11 injection. Bulk RNA sequencing was performed on LV tissue at 1, 3 and 6 hours following injection of rmIL11 and compared to controls injected with saline.

Extensive and significant transcription changes were apparent at all timepoints (**1hr,** Up:145, Down:27; **3hr,** Up: 450, Down: 303; **6hr:** Up: 268, Down: 169**;** $Log_2FC+/-1$, FDR<0.05). Genes differentially regulated included early upregulation of acute inflammatory genes (*Il6, Il1b* and *Il33*), chemotactic factors such as (*Ccl2* and *Cxcl1*) and CM stress markers *(Nppb, Cnn2, Ankrd1)* [**Fig 2A, B**]. Kyoto Encyclopedia of Genes and Genomes (KEGG) analysis of the differentially expressed genes at the 1-hour time point revealed the tumour necrosis factor α (TNFα), NF-κB and Janus kinase (JAK)/STAT signalling were among the most significantly enriched terms [**Fig 2C & Suppl Fig S2A, C]**. A similar group of inflammatory terms were highlighted by Hallmark Gene Set Enrichment Analysis including TNFα signalling via NFκB, IL6 JAK/STAT and interferon-gamma signalling [**Fig 2D & Suppl Fig S2B, D]**. These transcriptional changes show that IL11 drives an acute proinflammatory response in the heart that is associated with impaired systolic function.

**[Insert Figure 2]**

## Single nuclear sequencing reveals a cardiomyocyte stress signature

To examine cell-specific transcriptional responses and define any potential changes in cell populations, we performed single nucleus RNA-sequencing (snRNAseq) experiments on hearts 3 hours post rmIL11 injection [**Fig 3A, Suppl Fig S3A-C, S4A & Suppl Table 4]**. This revealed no significant change in cell populations overall, excluding immune cell infiltration at this early time point [**Fig 3B]** although chronic IL11 expression is known to cause immune cell infiltration[18].

On closer analysis of CMs, this cell type segregated into four states with rmIL11-treated CM predominantly clustered in state 0 [**Fig 3C, D]**. This state is defined by the expression of a number of cardiomyocyte stress factors including *Ankrd1*, *Ankrd23* and *Xirp2* [**Figure 3E & Suppl Fig S4B]**. *Ankrd1* and *Ankrd23* are stress-inducible ankyrin repeat proteins which are elevated in

dilated cardiomyopathies[26,27]. *Xirp2* encodes cardiomyopathy-associated protein 3 and is upregulated in CMs in response to stress[28,29]. Expression of *Nppb*, a canonical heart failure gene, was similarly elevated [**Fig 3E]**. Overall, the most enriched pathway from KEGG analysis of CM-specific differentially expressed genes, irrespective of state, was "Ribosome" with 93 out of 130 genes significantly upregulated (Fold enrichment:4.5, FDR:2.3e-46), perhaps related to the large effects of IL11 on protein translation within CMs to cellular stress [**Suppl Fig S5]**[30].

**[Insert Figure 3]**

## ATAC-Seq highlights AP-1 family genes

To better understand the molecular changes induced by IL11 in the heart, we performed an assay for transposase-accessible chromatin using sequencing (ATAC-seq) analysis. This methodology identifies regions of the genome undergoing epigenetic variation to make transcription factor binding sites more or less accessible.

Following IL11 administration, there were a large number of loci with variation in DNA accessibility (increased: 945; reduced**:** 445, shrunkenLog2FC:+/-0.3, Padj<0.1) [**Fig 4A & Suppl Table 5]**. The top twenty most differentially enriched regions [**Fig 4B, C]** include areas adjacent to *Ankrd1* and *Nppb*, stress genes that we had already found to be upregulated in CMs by snRNAseq at the same timepoint [**Fig 3E**, **Fig 4B & Suppl Table 4**].

DNA motif analysis of sequences captured by ATAC-seq, revealed the most enriched motifs after rmIL11 treatment were targets for FOSL2 and JUNB transcription factors [**Fig 4D & Suppl Table 6]**. These transcription factors belong to the activator protein-1 (AP-1) transcription factor family, which is important for CM stress responses, cardiac inflammation and fibrosis.[31,32] Notably, the STAT3 binding motif was also highly enriched.

We revisited our bulk RNA-seq data to examine the expression of the AP-1 transcription factor family transcripts after rmIL11 injection. This revealed that almost all of the AP-1 family transcripts are upregulated in the heart after rmIL11 injection [**Fig 4E]**. We then queried the snRNA-seq data and observed that *Fosl2*, *Junb*, *Atf6*, *Jun*, *Atf3* and *Mafg* are all significantly differentially expressed in CMs following rmIL11 injection [**Fig 4E and Suppl Table 4]**.

**[Insert Figure 4]**

## Viral-mediated CM-specific deletion of *Il11ra1*

Given that profound transcriptional changes occur across multiple cell types in the myocardium we sought to isolate the effects of IL11 on the CM and test whether the acutely negative inotropic effects of IL11 and CM stress signature are specifically mediated via IL11 activity in CMs. We proceeded to conditionally delete *Il11ra1* in CMs in the adult mouse using an AAV9 vector to express *Tnnt2*-dependent *Cre*-recombinase in CMs of *Il11ra1* floxed mice, which effectively removed the floxed exons to generate mice with viral-mediated deletion of *Il11ra1* in CMs (vCMKO mice) [**Fig 5A, B]**. Effective transfection in the myocardium was confirmed by immunoblotting for GFP which is co-expressed with the *Cre*-recombinase [**Fig 5C**]. Notably, vCMKO mice had diminished myocardial p-STAT3 following injection of rmIL11, confirming IL11 activation of JAK/STAT3 in CMs [**Fig 5C, D]**.

As compared to mice injected with saline, WT mice injected with rmIL11 had reduced LVEF (WT+rmIL11: 26.5% ± 3.6), whereas vCMKO injected with rmIL11 had a mean LVEF (vCMKO+rmIL11: 50.8% ± 2.7) that was indistinguishable from saline-injected controls (WT + saline: 64.2% ± 1.6; vCMKO + saline: 57.0%±4.0, n=3-5 per group) [**Fig 5E**]. Similar changes were seen in GCS (WT+saline: -33.4% ± 1.3; vCMKO+saline: -25.5% ± 1.9; vCMKO+rmIL11: -

24.6% ± 1.4; WT+rmIL11: -11.1% ± 1.0, p<0.0001) and VTI in the aortic arch (WT+saline: 37.8 mm ± 2.0; vCMKO+saline: 37.8 mm ± 1.9; vCMKO+rmIL11: 35.2 mm ± 4.03; WT+rmIL11: 21.3 mm ± 1.31, p<0.0371) [**Fig 5F, G]**. Interestingly, this experimental model still developed tachycardia following IL11 treatment, as seen in WT mice [**Fig 5H]**.

We performed experiments in CMs isolated from adult vCMKO mice. Unlike CMs isolated from WT animals [**Fig 1J, K]**, CM from vCMKO mice did not have a reduction in cell shortening in response to stimulation with rmIL11, as compared to unstimulated cells. Similarly, peak calcium concentration was not blunted by rmIL11 in vCMKO CMs **[Fig 5I, J].** As such, ILl1 effects in CMs are dependent on *Il11ra1* expression in CMs.

**[Insert figure 5]**

## Germline deletion of *Il11ra1* in cardiomyocytes

To strengthen the finding from the initial receptor knockout experiment that negative inotropic effects of IL11 are direct receptor-dependent effects on CMs, we used a complementary, germline deletion methodology. We crossed *Il11ra1* flox mice with *Myh6*-Cre (m6CMKO) mice[33] [**Fig 6A]** which achieved a more pronounced and consistent knockdown of *Il11ra1* that enabled experiments to be scaled across sexes [**Fig 6B]**. As seen in the vCMKO strain, m6CMKO mice of both sexes had reduced p-STAT3 following rmIL11 injection, which further established effective *Il11ra1* locus recombination in this strain and reaffirmed IL11-specific signalling in CMs [**Fig 6C, D]**.

Having established the m6CMKO strain, we examined the effects of rmIL11 on cardiac function in these mice [**Suppl Table 7]**. When injected with rmIL11, control mice (*Il11ra1*$^{fl/fl}$, *Myh6*-Cre$^{-/-}$) had significantly reduced LVEF whereas the LVEF of m6CMKO mice (*Il11ra1*$^{fl/fl}$,

*Myh6*-Cre$^{+/-}$) was similar to that of m6CMKO mice injected with saline [**Fig 6E]**. Similarly, following rmIL11 injection, GCS and VTI in the aortic arch were reduced in control mice expressing *Il11ra1* but not in m6CMKO mice **[Fig 6F, G].** It was evident that the molecular and cardiovascular phenotypes of m6CMKO mice injected with rmIL11 largely replicated those observed in the vCMKO mice. However, unlike the vCMKO strain, m6CMKO mice were protected against IL11-induced tachycardia [**Fig 6H]**.

In molecular studies of myocardial extracts, *Nppb* and *Fosl2*, the most strongly upregulated CM specific AP-1 transcript, were upregulated in *Il11ra*$^{fl/fl}$ control mice in response to rmIL11 injection but this was not seen in m6CMKO mice [**Fig 6I, J]**.

**[Insert Figure 6]**

## JAK inhibition protects against IL11-induced cardiac dysfunction

Canonical IL11 signalling through the IL11RA/gp130/JAK/STAT3 pathway has recently been implicated in the acute pro-inflammatory effects of IL11[34] and activation of STAT3 in the heart was immediate and pronounced following IL11 injection [**Fig 1I**]. To determine the functional relevance of JAK/STAT3 activation in the heart we pretreated mice with ruxolitinib (30 mg/kg), which inhibits JAK1/2 activation, prior to injection of rmIL11 [**Fig 7A]**.

We confirmed that administration of ruxolitinib at 30 mg/kg prevented activation of JAK/STAT3 signalling by immunoblotting [**Fig 7B]**. Having established the efficacy of ruxolitinib we studied its effect on cardiac physiology in 8 week old wild type male C57BL/6J mice injected with rmIL11. Ruxolitinib alone had no effect on LV function [**Fig 7C]**. Following injection of rmIL11, and as compared to buffer injected controls, mice pretreated with ruxolitinib had better

LVEF (Ruxo + rmIL11: 60.5% ± 2.79; Veh + rmIL11: 35.2% ± 0.79, p=0.0005, n=4), GCS (Ruxo + rmIL11: -27.1% ± 1.56; Veh + rmIL11: -13.6% ± 1.44, p=0.0009, n=4) and aortic VTI (Ruxo + rmIL11: 39.2 mm ± 10.9; Veh + rmIL11: 23.4 mm ± 1.92, p=0.0001, n=4) [**Fig 7C-E])**. Ruxolitinib pretreatment also prevented rmIL11-induced tachycardia (Ruxo + rmIL11: 497 ± 6.8; Veh + rmIL11: 419 ± 14.1, p=0.0008, n=4) [**Fig 7F]**. As seen with m6CMKO, JAK inhibition prevented stress-associated transcriptional changes in the heart of *Nppb* and *Fosl2* [**Fig 7G, H]**.

To exclude off-target effects and to replicate findings, the study was repeated with a second JAK inhibitor (tofacitinib, 20 mg/kg). As seen with ruxolitinib, pretreatment with tofacitinib protected against the varied deleterious effects of IL11 on cardiac function compared to vehicle-treated controls: LVEF (Tofa + rmIL11: 59.0% ± 4.2, p=0.0007), GCS (Tofa + rmIL11: -25.7% ± 2.1, p=0.002), VTI in the aortic arch (Tofa + rmIL11: 40.5 mm ±1.36, p<0.0001), and tachycardia (Tofa + rmIL11: 401 bpm ± 6.23, p=0.0002) [**Fig 7C-E]**.

**[Insert Figure 7]**

# Discussion

In some healthcare systems, rhIL11 is used routinely to increase platelet counts in patients with thrombocytopenia but this can cause serious cardiac complications that are unexplained and until now dismissed as non-specific. RhIL11 has also been trialled in a different context, as a cytoprotective agent, in patients across a range of other medical conditions (e.g. colitis, myocardial infarction, arthritis, cirrhosis), **[Table 1 & Supl Table 1]** as IL11 was previously thought to be anti-inflammatory and anti-fibrotic[16]. As such, many thousands of patients have received, and continue to receive, rhIL11 in clinical trials and as part of routine medical care. Long-acting formulations of rhIL11 have recently been devised and new clinical trials of rhIL11 are proposed[5].

While unexplained, the cardiac side effects of rhIL11 have long been recognised and a small clinical trial was initiated in 2009 to determine if rhIL11 (50 µg/kg) affected cardiac conduction (NCT00886743). This trial was terminated prematurely at the request of the sponsor and no formal conclusions were made. Other studies looking at the effects of injection of human IL11 to adult rats showed no effects on cardiac phenotypes and studies of human atrial myocytes were similarly negative[35,36]. We suggest that, for these reasons, the severe cardiac side effects of rhIL11 therapy have been explained away as indirect, non-specific effects and thus sidelined[36].

The findings of this study redress the earlier literature on IL11 activity in the heart where it was believed to be anti-fibrotic[14], which appears inaccurate[30], and that it was cytoprotective in CMs[13–15], which we challenge here.

We found that injection of species-matched rmIL11 to mice caused acute and dose-dependent LV impairment that was mediated via IL11's action in IL11RA1 expressing CMs. In response to rmIL11 exposure, CMs develop a 'stressed' phenotype with genes including *Ankrd1, Ankrd23, Xirp2* and *Nppb).* This mirrors transcriptional changes in human CMs from the border zone of myocardial infarcts[37]. In these studies, using pseudotime analysis, 'prestressed' CMs expressed *ANKRD1* and the subsequent emergence of AP-1 transcription factors such as *ATF3* and upregulation of their target genes herald the transition from pre-stressed to stressed state accompanied by expression of *NPPB.*

Powerful enrichment of the AP-1 family of transcription factors following rmIL11 injection was seen in bulk RNA-seq, snRNA-seq and ATAC-seq and was dependent upon the CM IL11 receptor and JAK signalling. Upregulation of this family of transcription factors was unexpected and likely has detrimental effects in the mouse heart[31,38]. AP-1 family activation is not immediately downstream of IL11:IL11RA:gp130 signalling and thus, the early IL11-stimulated activation of JAK/STAT3 appears to upregulate AP-1 transcription factors in the CM, priming the cell to respond to stress signals. In the injured zebrafish heart, AP-1 contributes to sarcomere disassembly and regeneration[39], which is IL11-dependent[40], providing an evolutionary context for IL11-mediated effects in the heart[41]. Similarly, the increase in CM ribosomal proteins seen in the single-nuclei RNA sequencing data may be priming the cell for this process however in the absence of regenerative potential of these cells this does not proceed.

Our use of two mouse models of CM-specific *Il11ra1* deletion shows and replicates that the effects of rmIL11 on cardiac function are via direct cardiotoxic effects on CMs and are not

explained by changes in circulating volume, as has previously been suggested[36] or secondary effects on other organ systems. The models used in this study involved the administration of a single dose of rmIL11 however in clinical practice, courses of therapy can involve daily infusions of rhIL11 for up to 21 days between chemotherapy cycles which are likely to compound the effect on the heart, specifically on fibrotic pathologies that are slower to establish[30].

The mechanisms underlying the cardiac dysfunction, while localised to CMs, are likely multifactorial and a number of candidates may be considered. *Rrad* is one of the most strongly upregulated transcripts at 1 and 3 hours [**Suppl Fig S6A]**. The *Rrad* protein product, RAD-GTPase is a well-characterised L-type calcium channel inhibitor[42,43] and its upregulation has been described in human myocardial infarction under the control of the AP-1 family transcription factor *ATF3*[37]. In our studies *Rrad* expression is dependent on the CM IL11 receptor, as vCMKO, m6CMKO and JAKi prevent the IL11-induced upregulation of this transcript [**Suppl Fig S6B-E]**. Similarly, increased expression of acute phase alarmins S100A8 and S100A9 is seen 1 and 3 hours after rmIL11 injection [**Suppl Fig S6F, G]**. These genes have both been previously implicated in impairment of CM calcium flux and myocardial depression in the setting of acute inflammation[44]. These candidates, and others, may be considered for investigation in follow-on studies.

There are several limitations to our study. The discrepancy between the tachycardia seen in vCMKO but not m6CMKO mice was not explored. Mice developed a marked tachycardia in response to rmIL11 therapy that can cause changes in ventricular function. It was not possible to isolate the effect of IL11 on ventricular function without the concurrent tachycardia however LVEF will typically increase in response to elevated heart rates. In some cases where tachycardia

is profound end-diastolic volume and therefore stroke volume can be decreased due to the shortened filling time. However, in our study the end diastolic volume increased after rmIL11 administration [**Table 2]** suggesting tachycardia was unlikely to play a major role in the change in cardiac output and studies in unloaded and paced CMs *ex vivo* provide orthogonal evidence of IL11 pathobiology on myocyte contraction and relaxation. It is known that IL11 is produced endogenously in the heart in mice following transverse aortic constriction and angiotensin II infusion[45] and in humans with atrial fibrillation[46] and heart failure[47]. However, whether endogenous IL11 is toxic to CMs and negatively inotropic in heart failure syndromes is not known and we cannot extrapolate from the data seen with acute, high dose injection of recombinant protein. The cardiac side effects associated with IL11 include arrhythmias (notably atrial fibrillation and flutter) that we did not study here.

In conclusion, we show for the first time that injection of IL11 at doses equivalent to those used in clinical practice causes IL11RA-dependent, CM-specific toxicities and acute heart failure. These data likely explain the serious cardiac side effects that occur with rhIL11 therapy. Previous studies in human and non-human primates have shown an association between IL11 administration and heart failure symptoms, myocardial hypertrophy and elevation in natriuretic peptides[5,47]. These associations combined with our data mechanistic data strongly question the ongoing use of rhIL11, and its further development, in patients with thrombocytopenia while identifying novel toxic effects of IL11 in the CM compartment of the heart.

# Funding:

This work was supported by the Wellcome Trust [203928/Z/16/Z to MS]; Foundation Leducq [16 CVD 03 to SAC]; the Medical Research Council (UK) [MC-A654-5QB30 to SAC, MC-A654-5QB10 to DC]; the National Institute of Health and Care Research Biomedical Research Centre Imperial College London; the National Medical Research Council Singapore STaR award [NMRC/STaR/0011/2012 to SAC]; Goh Cardiovascular Research Award [Duke-NUS-GCR/2015/0014 to SAC]; Duke-NUS Signature Research Programme funded by the Ministry of Health, Singapore Ministry of Health's National Medical Research Council under its Singapore Translational Research Investigator Award [MOH-STaR21jun-0003 to DJH], Centre Grant scheme [NMRC CG21APR1006 to DJH]; and Collaborative Centre Grant scheme [NMRC/CG21APRC006 to DJH]; and the RIE2020/RIE2025 PREVENT-HF Industry Alignment Fund Pre-Positioning Programme [IAF-PP H23J2a0033 to DJH], administered by A*STAR.



# Author Contribution

MS, AW, WWL, KV, DJH, DC, NH, PJRB and SAC were involved in conceptualisation and design of the study. KO, CVH, KO CJR were involved with data collection and analysis of isolated cardiomyocytes experiments; MS, KO, CVH, ER, CNT and EPN were involved in protein and RNA analysis; MS, KO, CVH, CNT performed the animal experimentation; MS and ERJ performed and analysed the echocardiography data; IA and ML performed and analysed the RNA

sequencing experiments; HM an ELL performed the single nuclei RNA sequencing analysis. MS, DJH, DC, NH and SAC provided funding for the project; MS and SAC prepared the manuscript and all authors reviewed and revised the manuscript and agreed with the publication.

## Conflicts of interest

SAC is a co-inventor on a number of patent applications relating to the role of IL11 in human diseases that include the published patents: WO2017103108, WO2017103108 A2, WO 2018/109174 A2, WO 2018/109170 A2. SAC is also a co-founder and shareholder of Enleofen Bio PTE LTD and VVB PTE LTD.

# References


1. Paul SR, Bennett F, Calvetti JA, Kelleher K, Wood CR, O'Hara RM Jr, Leary AC, Sibley B, Clark SC, Williams DA, et al. Molecular cloning of a cDNA encoding interleukin 11, a stromal cell-derived lymphopoietic and hematopoietic cytokine. *Proc Natl Acad Sci USA.* 1990;**87**:7512–7516.

2. Neben TY, Loebelenz J, Hayes L, McCarthy K, Stoudemire J, Schaub R, Goldman SJ. Recombinant human interleukin-11 stimulates megakaryocytopoiesis and increases peripheral platelets in normal and splenectomized mice. *Blood*. 1993;**81**:901–908.

3. Zhang J-J, Zhao R, Xia F, Li Y, Wang R-W, Guan X, Zhu J-G, Ma A-X. Cost-effectiveness analysis of rhTPO and rhIL-11 in the treatment of chemotherapy-induced thrombocytopenia in hematological tumors based on real-world data. *Ann Palliat Med.* 2022;**11**:2709–2719.

4. Kaye JA. FDA licensure of NEUMEGA to prevent severe chemotherapy-induced thrombocytopenia. *Stem Cells.* 1998;**16** Suppl 2:207–223.

5. Yu K-M, Lau JY-N, Fok M, Yeung Y-K, Fok S-P, Zhang S, Ye P, Zhang K, Li X, Li J, Xu Q, Wong W-T, Choo Q-L. Preclinical evaluation of the mono-PEGylated recombinant human interleukin-11 in cynomolgus monkeys. *Toxicol Appl Pharmacol*. 2018;**342**:39–49.

6. Nakagawa M, Owada Y, Izumi Y, Nonin S, Sugioka K, Nakatani D, Iwata S, Mizutani K, Nishimura S, Ito A, Fujita S, Daimon T, Sawa Y, Asakura M, Maeda M, Fujio Y, Yoshiyama M. Four cases of investigational therapy with interleukin-11 against acute myocardial infarction. *Heart Vessels*. 2016;**31**:1574–1578.

7. Nandurkar HH, Robb L, Tarlinton D, Barnett L, Köntgen F, Begley CG. Adult mice with targeted mutation of the interleukin-11 receptor (IL11Ra) display normal hematopoiesis. *Blood*. 1997;**90**:2148–2159.

8. Ng B, Widjaja AA, Viswanathan S, Dong J, Chothani SP, Lim S, Shekeran SG, Tan J, µgregor NE, Walker EC, Sims NA, Schafer S, Cook SA. Similarities and differences between IL11 and IL11RA1 knockout mice for lung fibro-inflammation, fertility and craniosynostosis. *Sci Rep*. 2021;**11**:14088.

9. Tanaka M, Hirabayashi Y, Sekiguchi T, Inoue T, Katsuki M, Miyajima A. Targeted disruption of oncostatin M receptor results in altered hematopoiesis. *Blood*. 2003;**102**:3154–3162.

10. Denton CP, Del Galdo F, Khanna D, Vonk MC, Chung L, Johnson SR, Varga J, Furst DE, Temple J, Zecchin C, Csomor E, Lee A, Wisniacki N, Flint SM, Reid J. Biological and clinical insights from a randomised phase II study of an anti-oncostatin M monoclonal antibody in systemic sclerosis. *Rheumatology*. 2023;**62**:1:234-242.

11. Smith JW 2nd. Tolerability and side-effect profile of rhIL-11. *Oncology*. 2000;**14**:41–47.

12. Liu N-W, Huang X, Liu S, Liu W-J, Wang H, Wang W, Lu Y. Elevated BNP caused by recombinant human interleukin-11 treatment in patients with chemotherapy-induced thrombocytopenia. *Support Care Cancer*. 2019;**27**:4293-4298.

13. Obana M, Miyamoto K, Murasawa S, Iwakura T, Hayama A, Yamashita T, Shiragaki M, Kumagai S, Miyawaki A, Takewaki K, Matsumiya G, Maeda M, Yoshiyama M, Nakayama H, Fujio Y. Therapeutic administration of IL-11 exhibits the postconditioning effects against

ischemia-reperfusion injury via STAT3 in the heart. *Am J Physiol Heart Circ Physiol.* 2012;**303**:H569–77.

14. Obana M, Maeda M, Takeda K, Hayama A, Mohri T, Yamashita T, Nakaoka Y, Komuro I, Takeda K, Matsumiya G, Azuma J, Fujio Y. Therapeutic activation of signal transducer and activator of transcription 3 by interleukin-11 ameliorates cardiac fibrosis after myocardial infarction. *Circulation*. 2010;**121**:684–691.

15. Kimura R, Maeda M, Arita A, Oshima Y, Obana M, Ito T, Yamamoto Y, Mohri T, Kishimoto T, Kawase I, Fujio Y, Azuma J. Identification of cardiac myocytes as the target of interleukin 11, a cardioprotective cytokine. *Cytokine*. 2007;**38**:107–115.

16. Cook SA, Schafer S. Hiding in Plain Sight: Interleukin-11 Emerges as a Master Regulator of Fibrosis, Tissue Integrity, and Stromal Inflammation. *Annu Rev Med.* 2020;**71**:263–276.

17. Corden B, Adami E, Sweeney M, Schafer S, Cook SA. IL-11 in cardiac and renal fibrosis: Late to the party but a central player. *Br J Pharmacol.* 2020;**177**:1695–1708.

18. Sweeney M, O'Fee K, Villanueva-Hayes C, Rahman E, Lee M, Vanezis K, Andrew I, Lim W-W, Widjaja A, Barton PJR, Cook SA. Cardiomyocyte-Restricted Expression of IL11 Causes Cardiac Fibrosis, Inflammation, and Dysfunction. *Int J Mol Sci.* 2023;**24**:12989.

19. Uhlén M, Fagerberg L, Hallström BM, Lindskog C, Oksvold P, Mardinoglu A, Sivertsson Å, Kampf C, Sjöstedt E, Asplund A, Olsson I, Edlund K, Lundberg E, Navani S, Szigyarto CA-K, Odeberg J, Djureinovic D, Takanen JO, Hober S, Alm T, Edqvist P-H, Berling H, Tegel H, Mulder J, Rockberg J, Nilsson P, Schwenk JM, Hamsten M, von Feilitzen K, Forsberg M, Persson L, Johansson F, Zwahlen M, von Heijne G, Nielsen J, Pontén F. Proteomics. Tissue-

based map of the human proteome. Science. 2015;347:1260419.

20. Human Protein Atlas. Tissue expression of IL11RA - Staining in heart muscle - The Human Protein Atlas [Internet]. [cited 2023 Nov 29];Available from: https://www.proteinatlas.org/ENSG00000137070-IL11RA/tissue/heart+muscle

21. Ng B, Dong J, Viswanathan S, Widjaja AA, Paleja BS, Adami E, Ko NSJ, Wang M, Lim S, Tan J, Chothani SP, Albani S, Schafer S, Cook SA. Fibroblast-specific IL11 signaling drives chronic inflammation in murine fibrotic lung disease. *FASEB J*. 2020;**34**:11802–11815.

22. Litviňuková M, Talavera-López C, Maatz H, Reichart D, Worth CL, Lindberg EL, Kanda M, Polanski K, Heinig M, Lee M, Nadelmann ER, Roberts K, Tuck L, Fasouli ES, DeLaughter DM, McDonough B, Wakimoto H, Gorham JM, Samari S, Mahbubani KT, Saeb-Parsy K, Patone G, Boyle JJ, Zhang H, Zhang H, Viveiros A, Oudit GY, Bayraktar OA, Seidman JG, Seidman CE, Noseda M, Hubner N, Teichmann SA. Cells of the adult human heart. *Nature*. 2020;**588**:466–472.

23. Litvinukova M, Lindberg E, Maatz H, Zhang H, Radke M, Gotthardt M, Saeb-Parsy K, Teichmann S, Hübner N. Single cell and single nuclei analysis human heart tissue v1 [Internet]. 2018 [cited 2023 Aug 30];Available from: https://www.protocols.io/view/single-cell-and-single-nuclei-analysis-human-heart-x54v98pkml3e/v1

24. Sikkel MB, Francis DP, Howard J, Gordon F, Rowlands C, Peters NS, Lyon AR, Harding SE, MacLeod KT. Hierarchical statistical techniques are necessary to draw reliable conclusions from analysis of isolated cardiomyocyte studies. *Cardiovasc Res*. 2017;**113**:1743–1752.

25. Widjaja AA, Dong J, Adami E, Viswanathan S, Ng B, Pakkiri LS, Chothani SP, Singh BK, Lim WW, Zhou J, Shekeran SG, Tan J, Lim SY, Goh J, Wang M, Holgate R, Hearn A, Felkin LE, Yen PM, Dear JW, Drum CL, Schafer S, Cook SA. Redefining IL11 as a regeneration-limiting hepatotoxin and therapeutic target in acetaminophen-induced liver injury. *Sci Transl Med*. 2021;**13**:eaba8146.

26. Ling SSM, Chen Y-T, Wang J, Richards AM, Liew OW. Ankyrin Repeat Domain 1 Protein: A Functionally Pleiotropic Protein with Cardiac Biomarker Potential. *Int J Mol Sci.* 2017;**18**(7):1362.

27. Zhang N, Ye F, Zhou Y, Zhu W, Xie C, Zheng H, Chen H, Chen J, Xie X. Cardiac ankyrin repeat protein contributes to dilated cardiomyopathy and heart failure. *FASEB J.* 2021;**35**:e21488.

28. McCalmon SA, Desjardins DM, Ahmad S, Davidoff KS, Snyder CM, Sato K, Ohashi K, Kielbasa OM, Mathew M, Ewen EP, Walsh K, Gavras H, Naya FJ. Modulation of angiotensin II-mediated cardiac remodeling by the MEF2A target gene Xirp2. *Circ Res.* 2010;**106**:952–960.

29. Dewenter M, Pan J, Knödler L, Tzschöckel N, Henrich J, Cordero J, Dobreva G, Lutz S, Backs J, Wieland T, Vettel C. Chronic isoprenaline/phenylephrine vs. exclusive isoprenaline stimulation in mice: critical contribution of alpha1-adrenoceptors to early cardiac stress responses. *Basic Res Cardiol*. 2022;**117**:15.

30. Schafer S, Viswanathan S, Widjaja AA, Lim W-W, Moreno-Moral A, DeLaughter DM, Ng B, Patone G, Chow K, Khin E, Tan J, Chothani SP, Ye L, Rackham OJL, Ko NSJ, Sahib NE,

Pua CJ, Zhen NTG, Xie C, Wang M, Maatz H, Lim S, Saar K, Blachut S, Petretto E, Schmidt S, Putoczki T, Guimarães-Camboa N, Wakimoto H, van Heesch S, Sigmundsson K, Lim SL, Soon JL, Chao VTT, Chua YL, Tan TE, Evans SM, Loh YJ, Jamal MH, Ong KK, Chua KC, Ong B-H, Chakaramakkil MJ, Seidman JG, Seidman CE, Hubner N, Sin KYK, Cook SA. IL-11 is a crucial determinant of cardiovascular fibrosis. *Nature*. 2017;**552**:110–115.

31. Stellato M, Dewenter M, Rudnik M, Hukara A, Özsoy Ç, Renoux F, Pachera E, Gantenbein F, Seebeck P, Uhtjaerv S, Osto E, Razansky D, Klingel K, Henes J, Distler O, Błyszczuk P, Kania G. The AP-1 transcription factor Fosl-2 drives cardiac fibrosis and arrhythmias under immunofibrotic conditions. *Commun Biol*. 2023;**6**:161.

32. van Duijvenboden K, de Bakker DEM, Man JCK, Janssen R, Günthel M, Hill MC, Hooijkaas IB, van der Made I, van der Kraak PH, Vink A, Creemers EE, Martin JF, Barnett P, Bakkers J, Christoffels VM. Conserved NPPB+ Border Zone Switches From MEF2- to AP-1-Driven Gene Program. *Circulation*. 2019;**140**:864–879.

33. Agah R, Frenkel PA, French BA, Michael LH, Overbeek PA, Schneider MD. Gene recombination in postmitotic cells. Targeted expression of Cre recombinase provokes cardiac-restricted, site-specific rearrangement in adult ventricular muscle in vivo. *J Clin Invest*. 1997;**100**:169–179.

34. Widjaja AA, Chothani S, Viswanathan S, Goh JWT, Lim W-W, Cook SA. IL11 Stimulates IL33 Expression and Proinflammatory Fibroblast Activation across Tissues. *Int J Mol Sci*. 2022;**23**(16):8900.

35. Sartiani L, De Paoli P, Lonardo G, Pino R, Conti AA, Cerbai E, Pelleg A, Belardinelli L,

Mugelli A. Does recombinant human interleukin-11 exert direct electrophysiologic effects on single human atrial myocytes? *J Cardiovasc Pharmacol*. 2002;**39**:425–434.

36. Xu J, Ren J-F, Mugelli A, Belardinelli L, Keith JC Jr, Pelleg A. Age-dependent atrial remodeling induced by recombinant human interleukin-11: implications for atrial flutter/fibrillation. *J Cardiovasc Pharmacol*. 2002;**39**:435–440.

37. Kuppe C, Ramirez Flores RO, Li Z, Hayat S, Levinson RT, Liao X, Hannani MT, Tanevski J, Wünnemann F, Nagai JS, Halder M, Schumacher D, Menzel S, Schäfer G, Hoeft K, Cheng M, Ziegler S, Zhang X, Peisker F, Kaesler N, Saritas T, Xu Y, Kassner A, Gummert J, Morshuis M, Amrute J, Veltrop RJA, Boor P, Klingel K, Van Laake LW, Vink A, Hoogenboezem RM, Bindels EMJ, Schurgers L, Sattler S, Schapiro D, Schneider RK, Lavine K, Milting H, Costa IG, Saez-Rodriguez J, Kramann R. Spatial multi-omic map of human myocardial infarction. *Nature*. 2022;**608**:766–777.

38. Freire G, Ocampo C, Ilbawi N, Griffin AJ, Gupta M. Overt expression of AP-1 reduces alpha myosin heavy chain expression and contributes to heart failure from chronic volume overload. *J Mol Cell Cardiol*. 2007;**43**:465–478.

39. Beisaw A, Kuenne C, Guenther S, Dallmann J, Wu C-C, Bentsen M, Looso M, Stainier DYR. AP-1 Contributes to Chromatin Accessibility to Promote Sarcomere Disassembly and Cardiomyocyte Protrusion During Zebrafish Heart Regeneration. *Circ Res*. 2020;**126**:1760–1778.

40. Allanki S, Strilic B, Scheinberger L, Onderwater YL, Marks A, Günther S, Preussner J, Kikhi K, Looso M, Stainier DYR, Reischauer S. Interleukin-11 signaling promotes cellular

reprogramming and limits fibrotic scarring during tissue regeneration. *Sci Adv.* 2021;**7**:eabg6497.

41. Cook SA. The Pathobiology of Interleukin 11 in Mammalian Disease is Likely Explained by its Essential Evolutionary Role for Fin Regeneration. *J Cardiovasc Transl Res.* 2023;**16**:755-757

42. Ahern BM, Levitan BM, Veeranki S, Shah M, Ali N, Sebastian A, Su W, Gong MC, Li J, Stelzer JE, Andres DA, Satin J. Myocardial-restricted ablation of the GTPase RAD results in a pro-adaptive heart response in mice. *J Biol Chem*. 2019;**294**:10913–10927.

43. Papa A, Zakharov SI, Katchman AN, Kushner JS, Chen B-X, Yang L, Liu G, Jimenez AS, Eisert RJ, Bradshaw GA, Dun W, Ali SR, Rodriques A, Zhou K, Topkara V, Yang M, Morrow JP, Tsai EJ, Karlin A, Wan E, Kalocsay M, Pitt GS, Colecraft HM, Ben-Johny M, Marx SO. Rad regulation of CaV1.2 channels controls cardiac fight-or-flight response. *Nat Cardiovasc Res*. 2022;**1**:1022–1038.

44. Boyd JH, Kan B, Roberts H, Wang Y, Walley KR. S100A8 and S100A9 mediate endotoxin-induced cardiomyocyte dysfunction via the receptor for advanced glycation end products. Circ Res. 2008;102:1239–1246.1. Paul SR, Bennett F, Calvetti JA, Kelleher K, Wood CR, O'Hara RM Jr, Leary AC, Sibley B, Clark SC, Williams DA, et al. Molecular cloning of a cDNA encoding interleukin 11, a stromal cell-derived lymphopoietic and hematopoietic cytokine. *Proc Natl Acad Sci USA.* 1990;**87**:7512–7516.

45. Corden B, Lim W-W, Song W, Chen X, Ko NSJ, Su L, Tee NGZ, Adami E, Schafer S, Cook SA. Therapeutic Targeting of Interleukin-11 Signalling Reduces Pressure Overload-Induced

Cardiac Fibrosis in Mice. *J Cardiovasc Transl Res*. 2021;**14**(2):222-228

46. Cong X, Tian B, Zhu X, Zhang X, Gu W, Zhao H, Hao S, Ning Z. Interleukin-11 Is Elevated in Patients with Atrial Fibrillation, Correlates with Serum Fibrosis Markers, and Represents a Therapeutic Target for Atrial Fibrosis. *Cerebrovasc Dis* 2023:**52**(5):1–12.

47. Ye J, Wang Z, Ye D, Wang Y, Wang M, Ji Q, Huang Y, Liu L, Shi Y, Zeng T, Xu Y, Liu J, Jiang H, Lin Y, Wan J. Increased Interleukin-11 Levels Are Correlated with Cardiac Events in Patients with Chronic Heart Failure. *Mediators Inflamm* 2019;**2**:1575410.

# Tables Legends

**Table 1. Human clinical trials registered with clinicaltrials.gov using recombinant human interleukin 11.**

**Table 2. Echocardiographic measures of cardiac function in saline, rmIL11 or rmIL6 treated mice.**

Wild type C57BL/6J mice were injected with saline (2 uL/kg), rmIL11 (200 µg/kg) or rmIL6 (200 µg/kg) and echocardiographic measures were recorded under isoflurane anaesthesia after 2 hours. Values are presented as mean ± SEM. *Statistics: Comparison between groups by one-way ANOVA with Sidak's multiple comparisons unless otherwise indicated. Values marked with * were not normally distributed and therefore significance was tested using Mann-Whitney U test. P-values less than 0.05 are considered significant.* Abbreviations used **bpm**:, beats per minute, **LVEF**, left ventricular ejection fraction; **FS,** fractional shortening; **ESV,** end systolic volume; **EDV,** end diastolic volume; **GCS**, global circumferential strain; **GLS**, global longitudinal strain; **VTI**, velocity time integral from pulse wave doppler trace in the aortic arch.

# Figure Legends

**Figure 1. IL11 causes acute heart failure and impairs cardiomyocyte calcium handling.** Male C57BL/6J mice were injected with rmIL11 (200 µg/kg) (■), rmIL6 (200 µg/kg)(▲) or an equivalent volume of saline (2 µl/kg) (●). **(A)** Representative electrocardiogram traces were recorded under light anaesthesia, 2 hours after intraperitoneal (IP) injection of saline, rmIL11 or rmIL6. **(B)** Quantification of heart rate (n=5 per group). **(C)** Representative m-mode images from echocardiography performed 2 hours after injection of saline, rmIL11 or rmIL6. **(D)** Quantification of left ventricular ejection fraction (LVEF), **(E)** global circumferential strain (GCS) and **(F)** velocity time integral at the aortic arch (VTI) in each group (n=5 per group). **(G)** LVEF 2 hours after IP injection of rmIL11 to male mice at 0, 5, 10, 25, 50, 100 & 200 µg/kg (n=5 per dose). **(H)** LVEF at baseline, 1, 2 ,4, 6, and 24 hours and 7 days after IP injection of rmIL11 (200 µg/kg) (n=4 per timepoint). **(I)** Western blot of myocardial lysates from C57BL/6J male mice 0.5, 3, 6 and 24 hours after IP rmIL11 injection (200 µg/kg). Blots are probed for pSTAT3, total STAT3, pERK, total ERK, pJNK, total JNK and GAPDH. CMs isolated from male C57BL/6J mice were treated *in vitro* for 2 hours with media supplemented with rmIL11 (10ng/mL) or non-supplemented media (Cntrl) (n=3 mice, 20 cells per mouse) and assessed for **(J)** contractility (effective n=9.7) and **(K)** the systolic change of intracellular calcium concentration (effective n=12). *Statistics: One-way ANOVA with Sidak's multiple comparisons test. Significance denoted as *p<0.05, **p<0.01, ***p<0.001, ****p<0.0001.CM data: two level hierarchical clustering p-values denoted as ***<0.001).*

**Figure 2. Transcriptional changes in the myocardium following rmIL11 injection.** Volcano plot of all detected genes **(A)** 1 hour (n=3) and **(B)** 3 hours (n=4) after intraperitoneal injection of rmIL11 at 200 µg/kg. Red lines are drawn at Log2Fc of 1 and -1 and FDR of 0.05. **(C)** Chart of most significantly enriched KEGG terms from at 1-hour post injection of rmIL11 ranked by FDR. **(D)** Gene set enrichment analysis of the most highly enriched Hallmark gene sets from RNAseq data at 1 hour after injection of rmIL11 ranked by normalised enrichment score.

**Figure 3. Single nuclear RNA sequencing reveals an IL11-induced cardiomyocyte stress signature.** **(A)** UMAP embedding of all cell types from the left ventricle of male C57BL/6J mice 3 hours after intraperitoneal injection of rmIL11 (200 µg/kg) or an equivalent volume of saline (n=5). **(B)** Comparison of cellular composition of the left ventricle in rmIL11 treated mice compared to saline treated mice. **(C)** UMAP embedding of cardiomyocyte fraction. 4 distinct clusters are identified based on gene expression. **(D)** UMAP embedding of cardiomyocytes annotated with the treatment group. **(E)** UMAP embedding of cardiomyocyte fraction of saline or rmIL11 treated cardiomyocytes annotated with relative expression of *Nppb* and *Ankrd1*. **Abbreviations:** EC, endothelial cells.

**Figure 4. ATAC-Seq reveals a stress signature that occurs acutely in the myocardium after rmIL11 injection. (A)** Number of positively and negatively enriched genomic regions identified by ATAC-Seq analysis of the myocardium 3 hours after injection of rmIL11 (n=4). **(B)** Top 20 most strongly enriched DNA regions in ATAC-seq analysis and adjacent genes, when present (*Gene* - **chromosome**). **(C)** Top 20 most strongly negatively enriched DNA regions in ATAC-seq analysis and adjacent genes (*Gene* - **chromosome**). **(D)** De novo Homer motif analysis of ATAC-seq data most highly enriched motifs in myocardial samples. **(E)** Heatmap of AP-1 transcription factor family members from bulk RNA sequencing data of myocardium at baseline, 1, 3 and 6 hours after rmIL11 injection. Genes differentially expressed in cardiomyocytes in single nuclear RNA sequencing data are highlighted in **red**.

**Figure 5. Viral-mediated *Il11ra1* deletion in adult cardiomyocytes protects against IL11-driven cardiac dysfunction. (A)** Schematic of experimental design for AAV9 mediated delivery of *Tnnt2* promoter driven Cre-recombinase to male $Il11ra1^{fl/fl}$ or $Il11ra1^{+/+}$ mice. **(B)** QPCR of relative myocardial expression of *Il11ra1* in $Il11ra1^{+/+}$ or $Il11ra1^{fl/fl}$ injected with AAV9-Cre or vehicle. **(C)** Western blot from myocardial lysate following rmIL11 injection (200 µg/kg) in $Il11ra1^{+/+}$ or $Il11ra1^{fl/fl}$ treated with either

AAV9-Cre or saline (n=3). The membrane was probed with primary antibodies against GFP, pSTAT3, STAT3, and GAPDH. **(D)** Quantification of relative pSTAT3/STAT3 from (C). Echocardiographic assessment of vCMKO mice injected with rmIL11 (200 µg/kg) (▲) or saline (▲) were compared to WT mice injected with rmIL11 (200 µg/kg) (●) or saline (●). **(E)** Left ventricular ejection fraction, **(F)** global circumferential strain, **(G)** velocity time integral at the aortic arch and **(H)** heart rate were measured 2 hours after treatment (n=4). **(I)** Contractility and **(J)** peak calcium amplitude in CMs isolated from vCMKO mice and treated for 2 hours *in vitro* with rmIL11 containing media (●) (10 ng/mL) or normal media (●). *Statistics: One-way ANOVA with Sidak's multiple comparisons testing. Significance denoted as *p<0.05, **p<0.01, ***p<0.001,****p<0.0001. CM data: two level hierarchical clustering).*

**Figure 6. Germline deletion of *Il11ra1* in cardiomyocytes prevents IL11-induced cardiac toxicities.** **(A)** Breeding strategy to generate m6CMKO mice and litter-mate *Il11ra1*$^{fl/fl}$ controls. **(B)** QPCR of *Il11ra1* gene expression in *Il11ra1*$^{fl/fl}$ controls and m6CMKO mice compared to male wild type C57BL/6J controls. (n=4) **(C)** Westerns blot of phospho-STAT3 and total STAT3 signalling in male and female *Il11ra1*$^{fl/fl}$ controls and m6CMKO mice with and without rmIL11 treatment. **(D)** Quantification of relative pSTAT and STAT3 expression. Male and female m6CMKO mice (CM *Il11ra* -) were treated with saline (■) or rmIL11 (■) and compared to wild type mice (CM *Il11ra1* +) treated with saline (●) or rmIL11(●) (n=4). **(E)** LVEF, **(F)** GCS, **(G)** VTI in the aortic arch and **(H)** heart rate was measured 2 hours after rmIL11 injection. (n=4). QPCR analysis of relative expression of **(I)** *Nppb* and **(J)** *Fosl2* in the myocardium following rmIL11 treatment of m6CMKO mice and *Il11ra1*$^{fl/fl}$ control mice (n=4). *Statistics: Comparison between groups by two-way ANOVA with Sidak's multiple comparisons. p-values denoted as *<0.05, **<0.01, ***<0.001, ****<0.0001).*

**Figure 7. The acute toxic effects of rmIl11 are mediated via JAK/STAT signalling. (A)** Schematic of the pretreatment of wild type male C57BL/6J mice with JAKi or vehicle 30 mins before administration of

rmIL11 or saline. **(B)** Western blot of myocardial lysate from mice 1 hour after injection with saline or rmIL11 following pretreatment with a either Ruxolitinib (30 mg/kg) (Ruxo), tofacitinib (20 mg/kg) (Tofa), or vehicle (Veh). Membranes have been probed for pSTAT3, STAT3 and GAPDH (n=3). 2 hours after treatment mice had an echocardiogram performed under isoflurane anaesthesia which measured **(C)** left ventricular ejection fraction, **(D)** global circumferential strain, **(E)** VTI in the aortic arch and **(F)** heart rate (n=4) in mice treated with a combination of vehicle (Veh), ruxolitinib (Ruxo), or tofacitinib (Tofa) and rmIL11 or saline. **(G)** QPCR of *Nppb* and **(H)** *Fosl2* expression in myocardial tissue from combinations of ruxolitinib and rmIL11 treatments (n=3). *Statistics: Comparison between groups by one-way ANOVA with Sidak's multiple comparisons test. Significance denoted as denoted *p<0.05, **p<0.01, ****p<0.0001.*

| NCT Number | Title | Start Date | n | Status | Phase |
|---|---|---|---|---|---|
| **Thrombocytopenia** | | | | | |
| NCT03823079 | Comparison of Interleukin-11 and rhTPO for Recurrent Colorectal Cancer Patients With Thrombocytopenia | Feb-19 | 50 | Unknown status | 2 |
| NCT01663441 | A Phase IIIa Study of Genetically Modified Recombinant Human Interleukin-11 | Mar-15 | 62 | Completed | 3 |
| NCT02314273 | Effect of rhIL-11 in Patients With Thrombocytopenia for Childhood Acute Lymphocytic Leukaemia | Sep-11 | 120 | Completed | 4 |
| NCT00886743 | Study Evaluating The Effects Of Oprelvekin On Cardiac Repolarization In Subjects With Chemotherapy Induced Thrombocytopenia | Sep-09 | 19 | Terminated | 2 |
| NCT00493181 | Interleukin 11, Thrombocytopenia, Imatinib in Chronic Myelogenous Leukemia Patients | Oct-05 | 8 | Completed | 2 |
| **Coagulopathy** | | | | | |
| NCT00994929 | Efficacy and Safety of IL-11 in DDAVP Unresponsive | Jan-10 | 9 | Completed | 2 |
| NCT00524225 | IL-11 in Adults With Von Willebrand Disease Undergoing Surgery | Feb-08 | 3 | Terminated | 2 |
| NCT00524342 | IL-11 in Women With Von Willebrand Disease and Refractory Menorrhagia | Jan-08 | 7 | Completed | 2 |
| NCT00151125 | Phase II Study of IL-11 (Neumega) in Von Willebrand Disease | Jul-04 | 12 | Completed | 2 |
| **Inflammatory Bowel Disease** | | | | | |
| NCT00038922 | Study Evaluating rhIL-11 in Left-Sided Ulcerative Colitis | Jun-02 | - | Terminated | 1 |
| NCT00040521 | Study Evaluating rhIL-11 in Active Crohn's Disease | Apr-02 | - | Completed | 2 |
| **Other** | | | | | |
| NCT00012298 | Radiolabeled Monoclonal Antibody Plus Rituximab With and Without Filgrastim and Interleukin-11 in Treating Patients With Relapsed or Refractory Non-Hodgkin's Lymphoma | Apr-01 | 81 | Terminated | 1/2 |
| NCT03720340 | Interleukin-11 Can Prevent and Treat of Radioactive Oral Mucitis | Oct-18 | 300 | Unknown status | 3 |

**Table 1. Human clinical trials registered with clinicaltrials.gov using recombinant human interleukin 11.**

| | Saline (n=5) | rmIL11 (n=5) | rmIL6 (n=5) | Saline vs rmIL11 p-value | rmIL11 vs rmIL6 p-value |
|---|---|---|---|---|---|
| **Heart rate (bpm)** | 410 ± 6.9 | 544 ± 13 | 459 ± 16 | 0.0079* | 0.004 |
| **LVEF (%)** | 62.4 ± 1.9 | 32.6 ± 2.9 | 59.4 ± 3.8 | <0.001 | <0.001 |
| **FS** | 27.3 ± 0.89 | 11.3 ± 1.1 | 27.9 ± 2.3 | <0.001 | <0.001 |
| **ESV (µL)** | 21.5 ± 4.4 | 42.6 ± 4.4 | 23.7 ± 2.8 | 0.010 | 0.007 |
| **EDV (µL)** | 55.8 ± 9.3 | 63.3 ± 6.1 | 58.1 ± 2.7 | 0.522 | 0.462 |
| **Stroke volume (µL)** | 34.4 ± 5.0 | 20.6 ± 2.6 | 34.4 ± 2.4 | 0.039 | 0.004 |
| **GCS (%)** | -33.4 ± 1.3 | -10.6 ± 0.6 | -25.7 ± 1.1 | <0.001 | <0.001 |
| **GLS (%)** | -19.8 ± 1.5 | -12.3 ± 1.6 | -16.5 ± 1.4 | 0.010 | 0.086 |
| **VTI (mm)** | 39.4 ± 3.6 | 20.2 ± 2.1 | 35.4 ± 4.0 | 0.002 | 0.010 |

**Table 2. Echocardiographic measures of cardiac function in saline, rmIL11 or rmIL6 treated mice.**

Wild type C57BL/6J mice were injected with saline (2 uL/kg), rmIL11 (200 µg/kg) or rmIL6 (200 µg/kg) and echocardiographic measures were recorded under isoflurane anaesthesia after 2 hours. Values are presented as mean ± SEM. *Statistics: Comparison between groups by one-way ANOVA with Sidak's multiple comparisons unless otherwise indicated. Values marked with * were not normally distributed and therefore significance was tested using Mann-Whitney U test. P-values less than 0.05 are considered significant.* Abbreviations used **bpm**:, beats per minute, **LVEF**, left ventricular ejection fraction; **FS,** fractional shortening; **ESV,** end systolic volume; **EDV,** end diastolic volume; **GCS**, global circumferential strain; **GLS**, global longitudinal strain; **VTI**, velocity time integral from pulse wave doppler trace in the aortic arch.

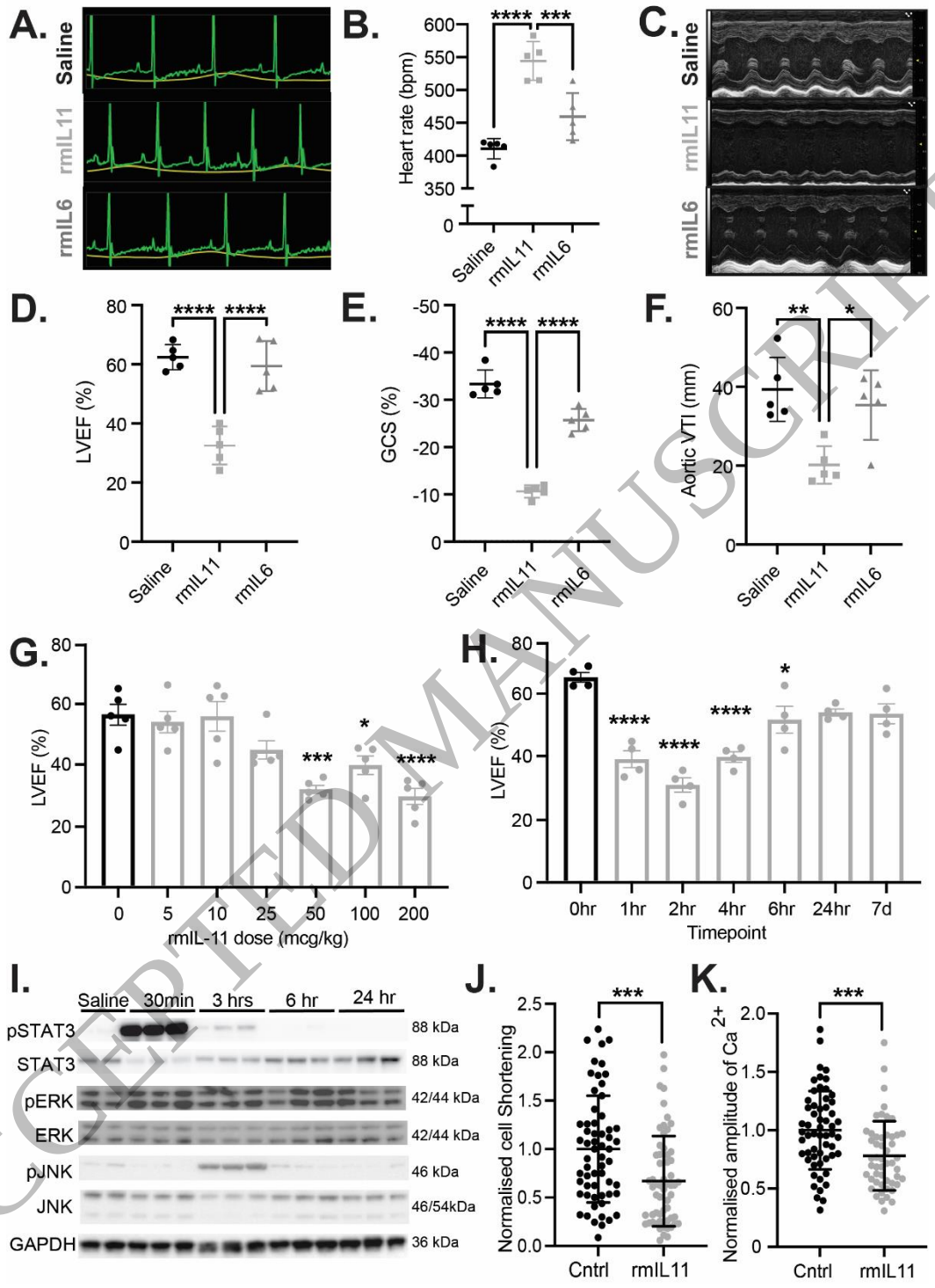


*Figure 1*
*174x242 mm ( x DPI)*

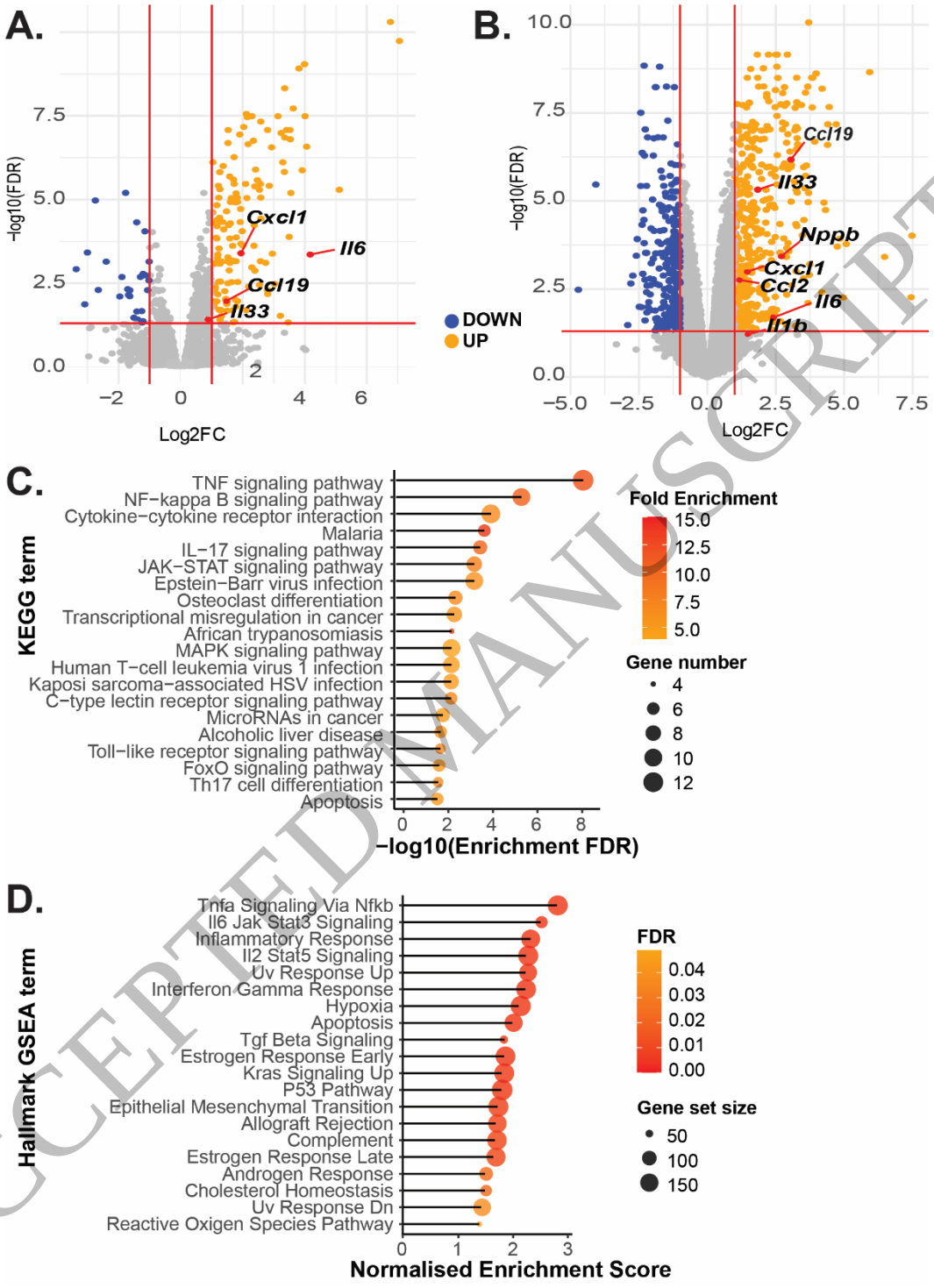


*Figure 2*
*174x241 mm ( x DPI)*

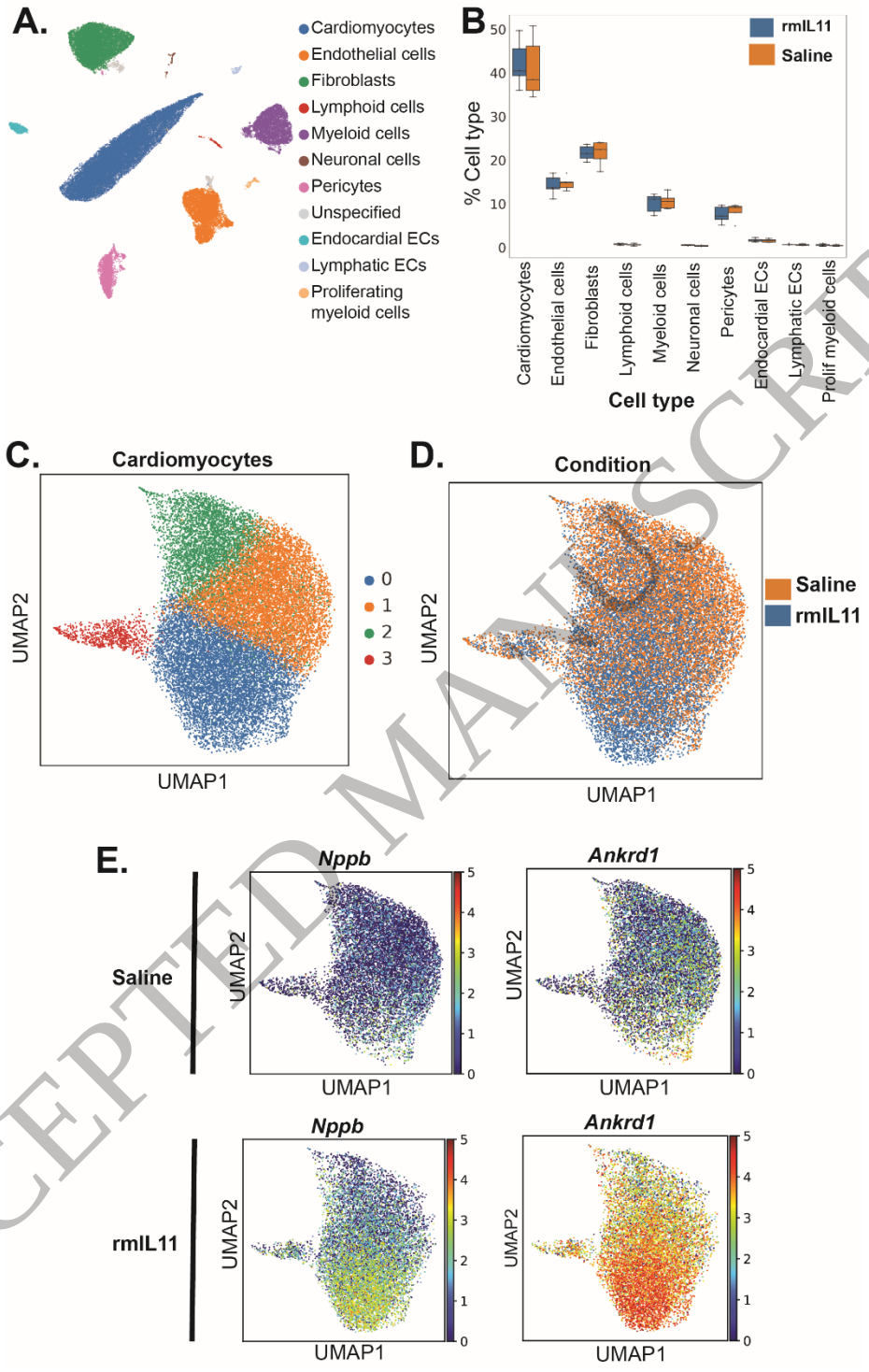


*Figure 3*
*175x279 mm ( x DPI)*

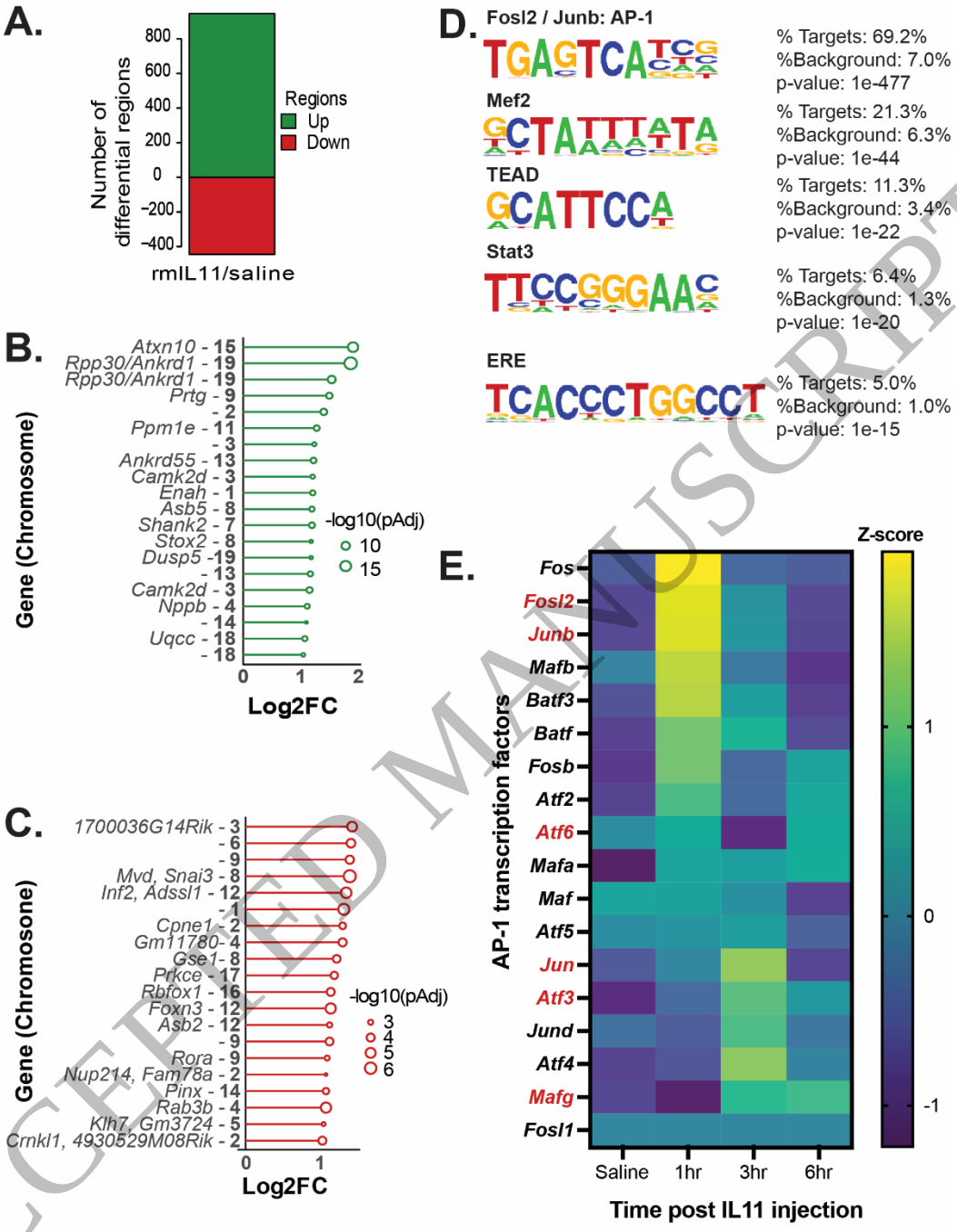


*Figure 4*
*173x224 mm ( x DPI)*

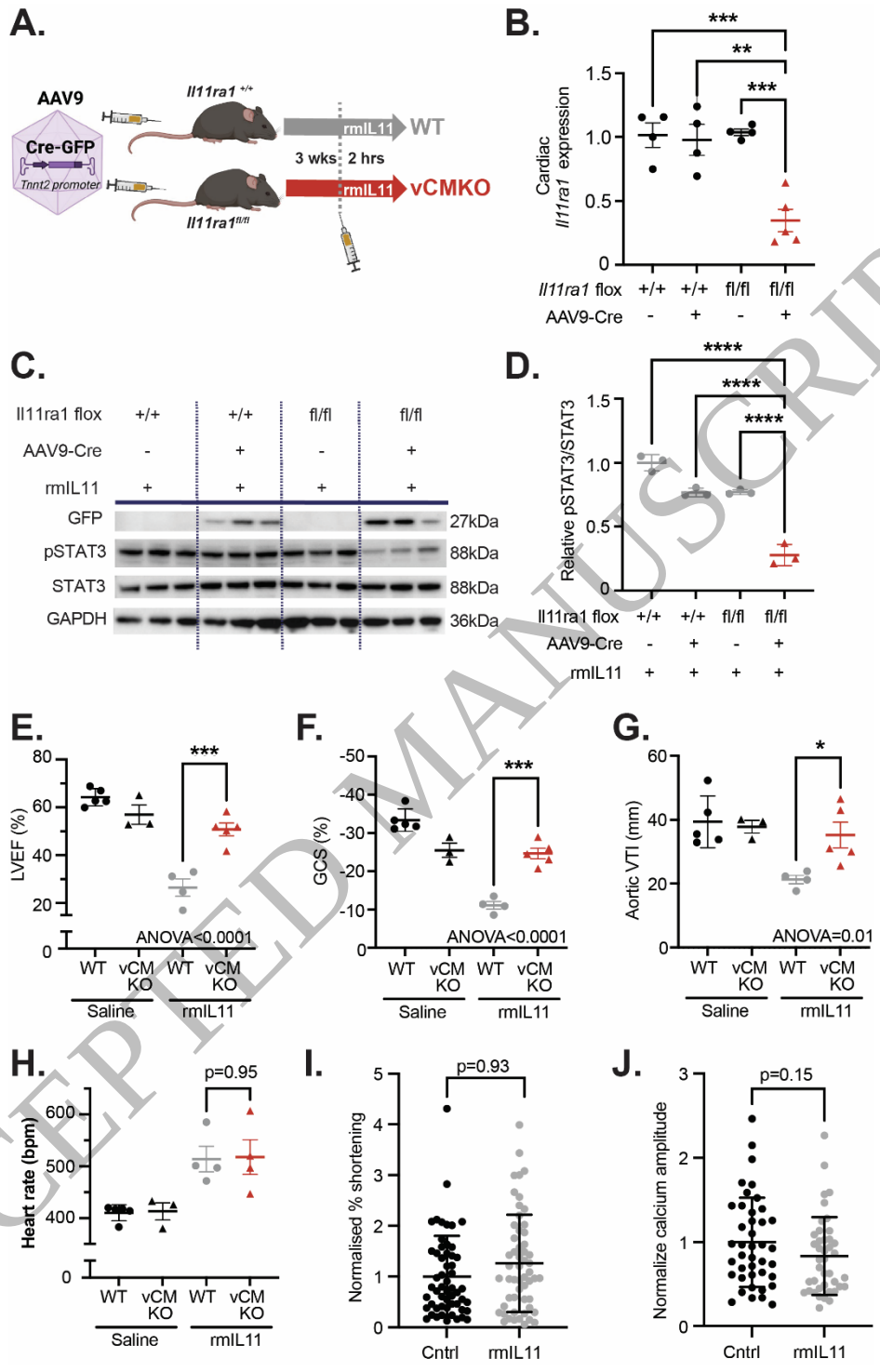


*Figure 5*
*173x272 mm ( x DPI)*

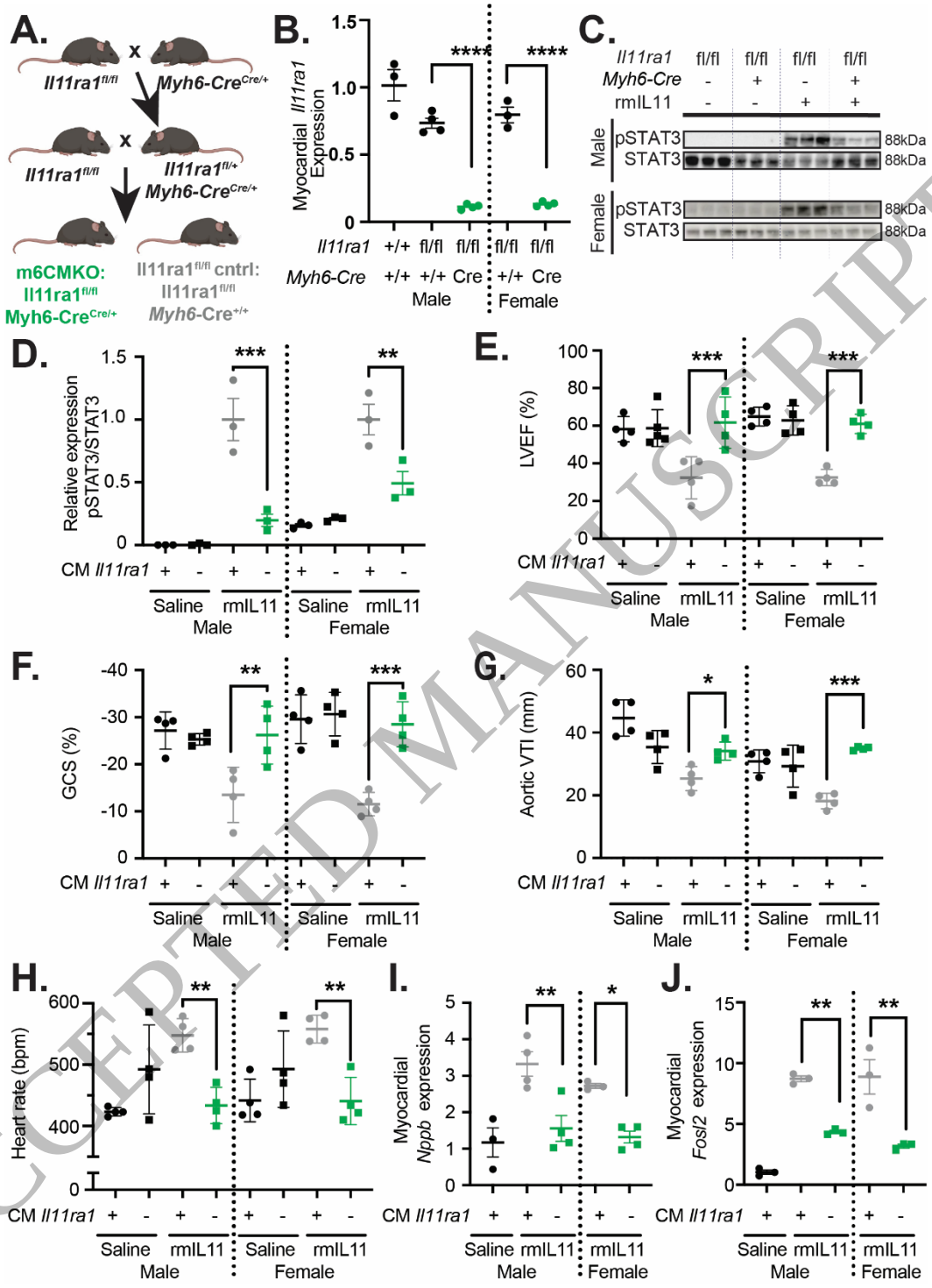


*Figure 6*
*175x243 mm ( x DPI)*

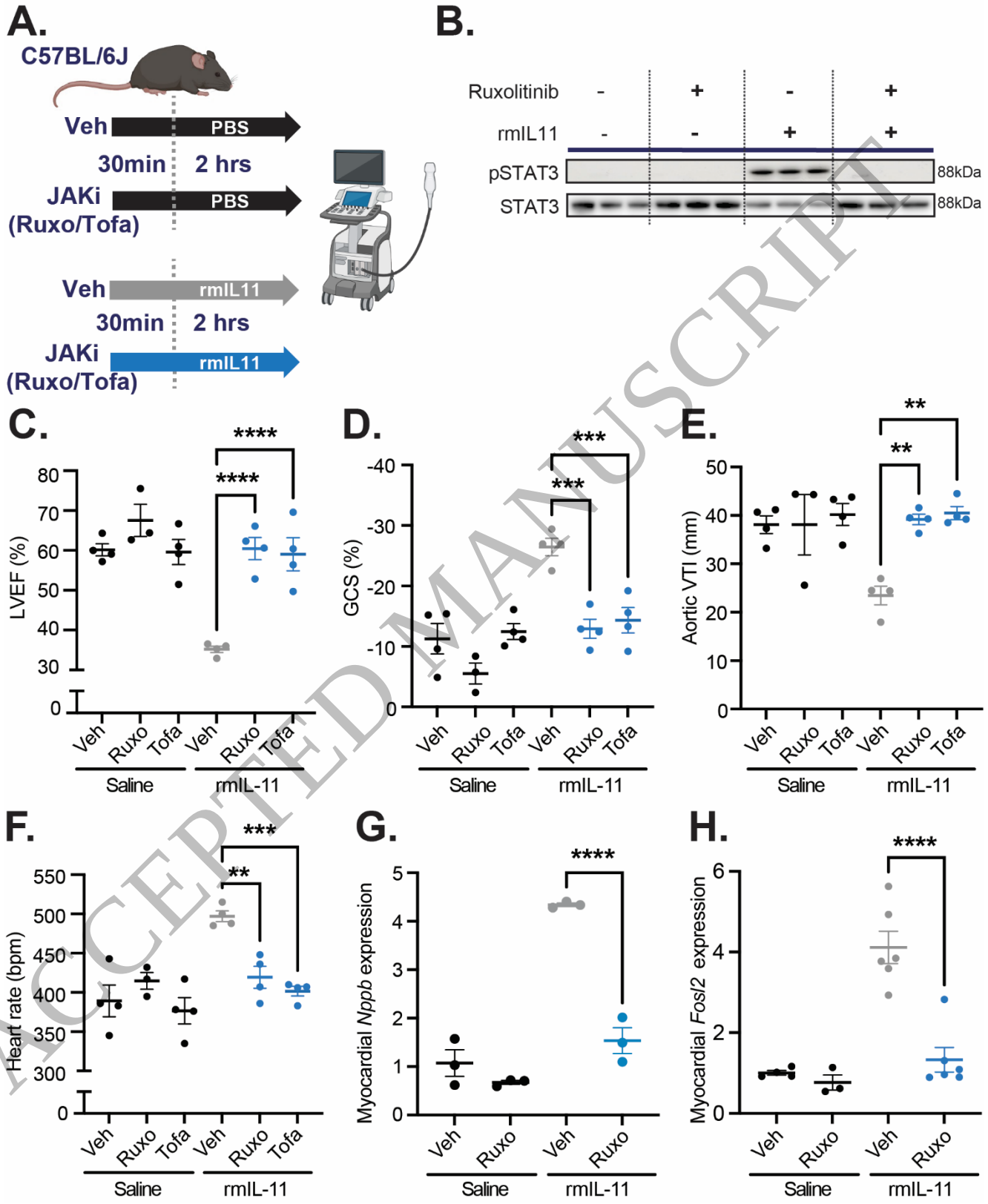


*Figure 7*
*175x214 mm ( x DPI)*

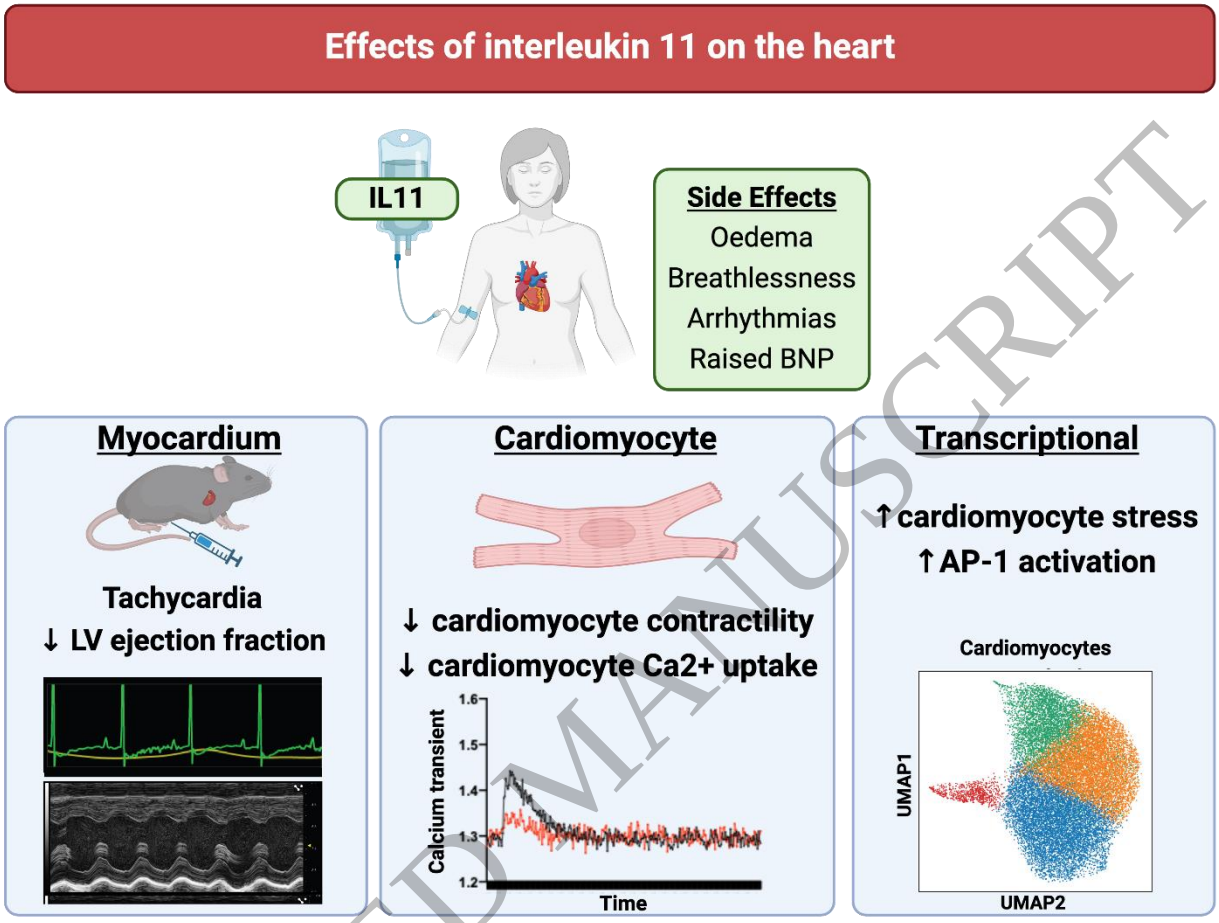


*Graphical Abstract*